P-06-187

Forsmark site investigation

Formation factor logging in situ by electrical methods in KFM07A and KFM08A

Martin Löfgren, Kemakta Konsult AB

September 2006

Svensk Kärnbränslehantering AB
Swedish Nuclear Fuel
and Waste Management Co
Box 5864
SE-102 40 Stockholm Sweden
Tel 08-459 84 00
+46 8 459 84 00
Fax 08-661 57 19
+46 8 661 57 19

ISSN 1651-4416
SKB P-06-187

Forsmark site investigation

Formation factor logging in situ by electrical methods in KFM07A and KFM08A

Martin Löfgren, Kemakta Konsult AB

September 2006

Keywords: AP PF 400-06-055, In situ, Formation factor, Rock resistivity, Electrical conductivity.

This report concerns a study which was conducted for SKB. The conclusions and viewpoints presented in the report are those of the author and do not necessarily coincide with those of the client.

A pdf version of this document can be downloaded from www.skb.se

Abstract

This report presents measurements and interpretations of the formation factor of the rock surrounding the boreholes KFM07A and KFM08A in Forsmark, Sweden. The formation factor was logged in situ by electrical methods.

For KFM07A, the in situ rock matrix formation factors obtained range from 1.7×10^{-5} to 2.9×10^{-4}. The in situ fractured rock formation factors obtained range from 1.7×10^{-5} to 6.7×10^{-4}. The obtained formation factor distributions deviate from the log-normal distribution. This may be due to the fact that details in the assessed electrical conductivity profile for the groundwater are questionable. The mean values and standard deviations of the obtained $\log_{10}$-normal distributions are –4.4 and 0.16, and –4.4 and 0.21 for the in situ rock matrix and fractured rock formation factor, respectively.

For KFM08A, the in situ rock matrix formation factors obtained range from 9.1×10^{-6} to 7.3×10^{-4}, whereas the in situ fractured rock formation factors obtained range from 8.9×10^{-6} to 3.8×10^{-3}. The distributions of the formation factors are in this case well described by the log-normal distribution. The mean values and standard deviations of the obtained $\log_{10}$-normal distributions are –4.5 and 0.17, and −4.4 and 0.22 for the in situ rock matrix and fractured rock formation factor, respectively.

When obtaining the electrical conductivity profiles of the groundwater in the boreholes, complementary data from other boreholes in the Forsmark area were used.

It should be noted that the pore water of the rock surrounding KFM07A appears to be more saline at and below repository depth than at other investigated locations within the Forsmark site investigation area.

Sammanfattning

Denna rapport presenterar mätningar och tolkningar av bergets formationsfaktor runt borrhålen KFM07A och KFM08A i Forsmark, Sverige. Formationsfaktorn har loggats in situ med elektriska metoder.

För KFM07A varierar den erhållna in situ formationsfaktorn för bergmatrisen från $1{,}7\times10^{-5}$ till $2{,}9\times10^{-4}$. Den erhållna in situ formationsfaktorn för sprickigt berg varierar från $1{,}7\times10^{-5}$ till $6{,}7\times10^{-4}$. De erhållna formationsfaktordistributionerna avviker från log-normal fördelningen. Detta kan vara en konsekvens av att detaljer i profilen för grund-vattnets elektriska konduktivitet, som tagits fram för borrhålet, kan ifrågasättas. Medelvärdena och standardavvikelserna för de erhållna $\log_{10}$-normalfördelningarna är
–4,4 och 0,16 samt –4,4 och 0,21 för in situ formationsfaktorn för bergmatrisen respektive sprickigt berg.

För KFM08A varierar den erhållna in situ formationsfaktorn för bergmatrisen från $9{,}1\times10^{-6}$ till $7{,}3\times10^{-4}$, medan den erhållna in situ formationsfaktorn för sprickigt berg varierar från $8{,}9\times10^{-6}$ till $3{,}8\times10^{-3}$. Formationsfaktorerna är i detta fall väl log-normalfördelade. Medelvärdena och standardavvikelserna för de erhållna $\log_{10}$-normalfördelningarna är –4,5 och 0,17 samt –4,5 och 0,22 för in situ formationsfaktorn för bergmatrisen respektive sprickigt berg.

För att erhålla profiler över grundvattnets elektriska konduktivitet i borrhålen användes kompletterande data från andra borrhål i Forsmarksområdet.

Det skall noteras att porvattnet i berget som omger KFM07A verkar vara mer salint vid och under förvarsdjup än på andra undersökta platser inom Forsmarks plats-undersökningsområde.

Contents

1 Introduction

This document reports the data gained from measurements of the formation factor of rock surrounding the boreholes KFM07A and KFM08A, within the site investigation at Forsmark. The work was carried out in accordance with activity plan AP PF 400-06-055. In Table 1-1 controlling documents for performing this activity are listed. Both activity plan and method description are SKB's internal controlling documents.

The formation factor was logged in situ by electrical methods. Other contractors performed the fieldwork, and that work is outside the framework of this activity. The interpretation of in situ data and compilation of formation factor logs were performed by Kemakta Konsult AB in Stockholm, Sweden.

Figure 1-1 shows the Forsmark site investigation area and the location of different drill sites. KFM07A and KFM08A are located at the drill sites DS7 and DS8, respectively.

Table 1-1. Controlling documents for performance of the activity.

Activity plan	Number	Version
Bestämning av formationsfaktorn från in situ resistivitets-mätningar i KFM07A och KFM08A	AP PF 400-06-055	1.0
Method description	**Number**	**Version**
Bestämning av formationsfaktorn med elektriska metoder	SKB MD 530.007	1.0

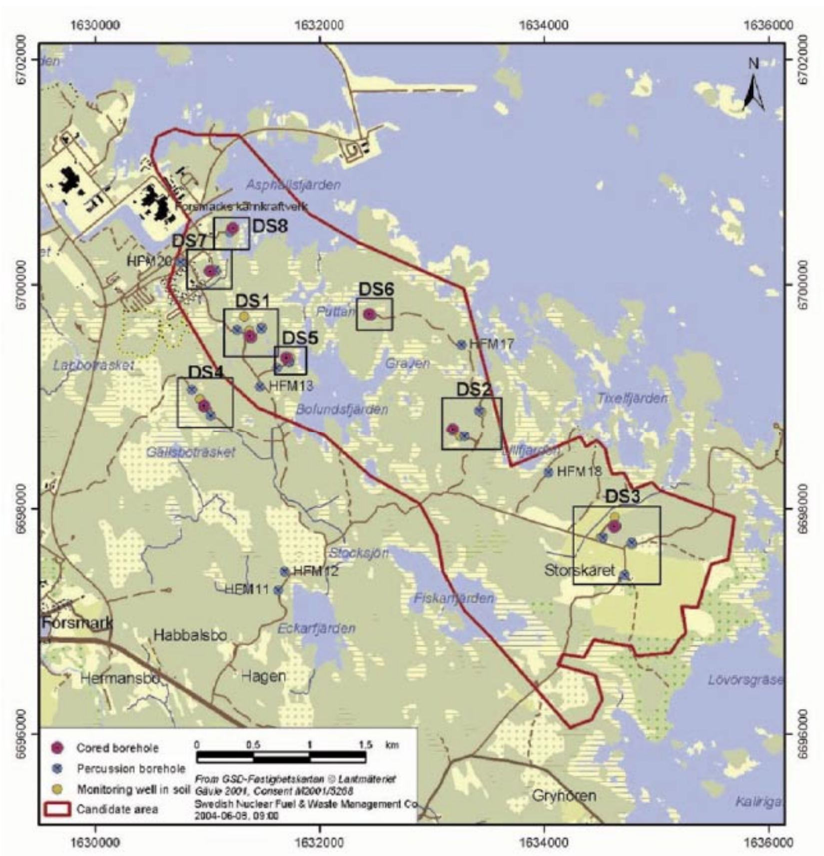

Figure 1-1. *General overview over the Forsmark site investigation area.*

2 Objective and scope

The formation factor is an important parameter that may be used directly in the safety assessment calculation of radionuclide transport in crystalline rock. The main objective of this work is to obtain the formation factor of the rock mass surrounding the boreholes KFM07A and KFM08A. This has been achieved by performing formation factor loggings by electrical methods in situ. The in situ method gives a great number of formation factors obtained under more natural conditions than in the laboratory. To obtain the in situ formation factor, results from previous loggings were used. Other contractors carried out the fieldwork.

3 Equipment

3.1 Rock resistivity measurements

The resistivity of the rock surrounding the boreholes KFM07A and KFM08A was logged using the focused rock resistivity tool Century 9072 /1/. The tool emits an alternating current perpendicular to the borehole axis from a main current electrode. The shape of the current field is controlled by electric fields emitted by guard electrodes. By using a focused tool, the disturbance from the borehole is minimised. The quantitative measuring range of the Century 9072 tool is 0–50,000 Ωm according to the manufacturer. The rock resistivity was also logged using the Century 9030 tool. However, this tool may not be suitable for quantitative logging in granitic rock and the results are not used in this report.

3.2 Groundwater electrical conductivity measurements

The EC (electrical conductivity) of the borehole fluid in KFM07A /2/ and KFM08A /3/ was logged using the POSIVA difference flow meter. The tool is shown in Figure 3-1.

When logging the EC of the borehole fluid, the lower rubber disks of the tool are not used. During the measurements, a drawdown can either be applied or not. Measurements were carried out before and after extensive pumping in boreholes KFM07A and KFM08A.

When using both the upper and the lower rubber disks, a section around a specific fracture can be packed off. By applying a drawdown at the surface, groundwater can thus be extracted from specific fractures. This is done in fracture specific EC measurements. By also measuring the groundwater flow out of the fracture, it is calculated how long time it will take to fill up the

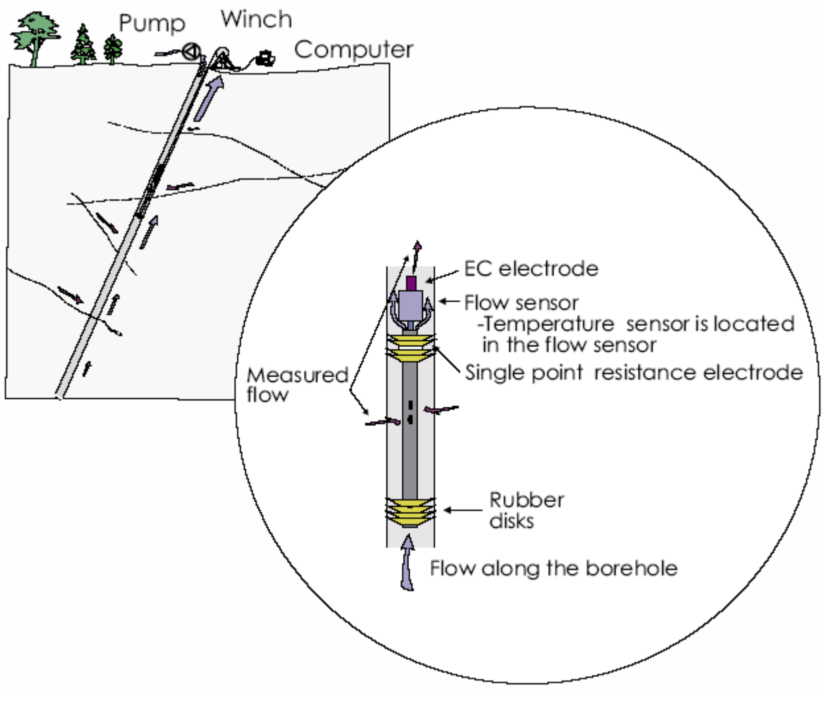

Figure 3-1. *Schematics of the POSIVA difference flow meter (image taken from /2/).*

packed off borehole section three times. During this time the EC is measured and a transient EC curve is obtained. After this time it is assumed that the measured EC is representative for the groundwater flowing out of the fracture. The measurements may be disturbed by leakage of borehole fluid into the packed off section and development of gas from species dissolved in the groundwater. Interpretations of transient EC curves are discussed in /4/. The quantitative measuring range of the EC electrode of the POSIVA difference flow meter is 0.02–11 S/m.

The EC, among other entities, of the groundwater coming from fractures in larger borehole sections is measured as a part of the hydrochemical characterisation. A section is packed off and by using a drawdown, groundwater is extracted from fractures within the section and brought to the surface for chemical analysis. A hydrochemical characterisation was performed in KFM07A /5/ as well s in KFM08A. The latter is not yet reported.

3.3 Difference flow loggings

By using the POSIVA difference flow meter, water-conducting fractures can be located. The tool, shown in Figure 3-1, has a flow sensor and the flow from fractures in packed off sections can be measured. When performing these measurements, both the upper and the lower rubber disks are used. Measurements can be carried out both with and without applying a drawdown. The quantitative measuring range of the flow sensor is 0.1–5,000 ml/min.

Difference flow loggings were performed in two different campaigns in KFM07A /2/ respectively KFM08A /3/.

3.4 Boremap loggings

The drill cores of KFM07A /6/ and KFM08A /7/ were logged together with a simultaneous study of video images of the borehole wall. This is called Boremap logging.

In the core log, fractures parting the core are recorded. Fractures parting the core that have not been induced during the drilling or core handling are called broken fractures. To decide if a fracture actually was open or sealed in the rock volume (i.e. in situ), SKB has developed a confidence classification expressed at three levels, “possible”, “probable” and “certain”, based on the weathering and fit of the fracture surfaces /7/. However, there is a strong uncertainty associated with determining whether broken fractures were open or not before drilling /8/. For this reason, it was decided to treat all broken fractures as potentially open in situ in this present report.

In the Boremap logging, parts of the core that are crushed or lost are also recorded, as well as the spatial distribution of different rock types.

4 Execution

4.1 Theory

4.1.1 The formation factor

The theory applied for obtaining formation factors by electrical methods is described in /9/. The formation factor is the ratio between the diffusivity of the rock matrix to that of free pore water. If the species diffusing through the porous system is much smaller than the characteristic length of the pores and no interactions occur between the mineral surfaces and the species, the formation factor is only a geometrical factor that is defined by the transport porosity, the tortuosity and the constrictivity of the porous system:

$$F_f = \frac{D_e}{D_w} = \varepsilon_t \frac{\delta}{\tau^2} \qquad \text{4-1}$$

where F_f (–) is the formation factor, D_e (m^2/s) is the effective diffusivity of the rock, D_w (m^2/s) is the diffusivity in the free pore water, ε_t (–) is the transport porosity, τ (–) is the tortuosity, and δ (–) is the constrictivity. When obtaining the formation factor with electrical methods, the Einstein relation between diffusivity and ionic mobility is used:

$$D = \frac{\mu RT}{zF} \qquad \text{4-2}$$

where D (m^2/s) is the diffusivity, μ ($m^2/V\times s$) is the ionic mobility, z (–) the charge number, and R ($J/mol\times K$), T (K) and F (C/mol) are the gas constant, temperature, and Faraday constant respectively. From the Einstein relation it is easy to show that the formation factor also is given by the ratio of the pore water resistivity to the resistivity of the saturated rock /10/:

$$F_f = \frac{\rho_w}{\rho_r} \qquad \text{4-3}$$

where ρ_w (Ωm) is the pore water resistivity and ρ_r (Ωm) is the rock resistivity. The resistivity of the saturated rock can easily be obtained by standard geophysical methods.

At present it is not feasible to extract pore water from the rock matrix in situ. Therefore, it is assumed that the pore water is in equilibrium with the free water surrounding the rock, and measurements are performed on this free water. The validity of this assumption has to be discussed for every specific site.

In a new line of experiments, species in the pore water in drill core samples brought to the laboratory are leached. This was done in KFM06A /11/ and the results from these measurements were used when validating the assumed electrical conductivity profile of the groundwater in KFM06A /12/. It was observed that the electrical conductivity profile obtained from in situ measurements, using the same methodology as in this present report, corresponded sufficiently well with data obtained by leaching drill cores samples.

The resistivity is the reciprocal to electrical conductivity. Traditionally the EC (electrical conductivity) is used when measuring on water and resistivity is used when measuring on rock.

4.1.2 Surface conductivity

In intrusive igneous rock the mineral surfaces are normally negatively charged. As the negative charge often is greater than what can be balanced by cations specifically adsorbed on the mineral surfaces, an electrical double layer with an excess of mobile cations will form at the pore wall. If a potential gradient is placed over the rock, the excess cations in the electrical double layer will move. This process is called surface conduction and this additional conduction may have to be accounted for when obtaining the formation factor of rock saturated with a pore water of low ionic strength. If the EC of the pore water is around 0.5 S/m or above, errors associated with surface conduction are deemed to be acceptable. This criterion is based on laboratory work by /13/ and /14/. The effect of the surface conduction on rock with formation factors below 1×10^{-5} was not investigated in these works. In this report, surface conduction has not been accounted for, as in general only the groundwater in the upper 100 or 200 m of the boreholes has a low ionic strength and as more knowledge is needed on surface conduction before performing corrections.

4.1.3 Artefacts

Comparative studies have been performed on a large number of 1–2 cm long samples from Äspö in Sweden /13/. Formation factors obtained with an electrical resistivity method using alternating current were compared to those obtained by a traditional through diffusion method, using Uranine as the tracer. The results show that formation factors obtained by the electrical resistivity measurements are a factor of about 2 times larger that those obtained by through diffusion measurements. A similar effect was found on granitic samples up to 12 cm long, using iodide in tracer experiments /15/. The deviation of a factor 2 between the methods may be explained by anion exclusion of the anionic tracers. Previously performed work suggests that the Nernst-Einstein equation between the diffusivity and electrical conductivity is generally applicable in granitic rock and that no artefacts give rise to major errors. It is uncertain, however, to what extent anion exclusion is related to the degree of compression of the porous system in situ due to the overburden.

4.1.4 Fractures in situ

In situ rock resistivity measurements are highly disturbed by free water in open fractures. The current sent out from the downhole tool in front of an open fracture will be propagated both in the porous system of the rock matrix and in the free water in the open fracture. Due to the low formation factor of the rock matrix, current may be preferentially propagated in a fracture intersecting the borehole if its aperture is on the order of 10^{-5} m or more.

There could be some confusion concerning the terminology of fractures. In order to avoid confusion, an organization sketch of different types of fractures is shown in Figure 4-1. The subgroups of fractures that interfere with the rock resistivity measurements are marked with grey.

The information concerning different types of fractures in situ is obtained from the interpretation of the Boremap logging and in the hydraulic flow logging. A fracture intersecting the borehole is most likely to part the drill core. In the core log, fractures that part the core are either broken or operational (drill-induced). Unbroken fractures, which do not part the core, are sealed or only partly open. Laboratory results suggest that sealed fractures generally have no major interference on rock resistivity measurements. The water-filled void in partly open fractures can be included in the porosity of the rock matrix.

Broken fractures are either interpreted as open or sealed. Open fractures may have a significant or insignificant aperture. An insignificant aperture represents an aperture so small that the amount of water held by the fracture is comparable with that held in the adjacent porous system. In this case the "adjacent porous system" concerns the porous system of the rock matrix within the first few centimetres from the fracture.

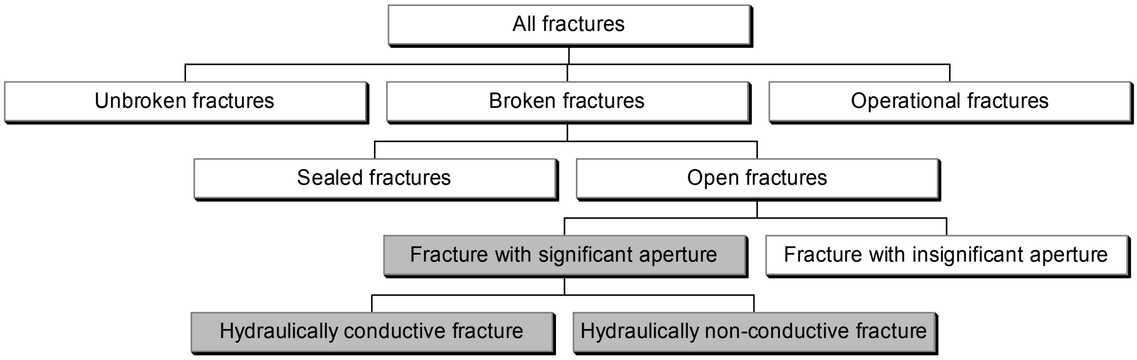

Figure 4-1. *Organization sketch of different types of fractures in situ.*

If the fracture has a significant aperture, it holds enough water to interfere with the rock resistivity measurements. Fractures with a significant aperture may be hydraulically conductive or non-conductive, depending on how they are connected to the fracture network.

Due to uncertainties in the interpretation of the core logging, all broken fractures are assumed to potentially have a significant aperture.

4.1.5 Rock matrix and fractured rock formation factor

In this report the rock resistivity is used to obtain formation factors of the rock surrounding the borehole. The obtained formation factors may later be used in models for radionuclide transport in fractured crystalline rock. Different conceptual approaches may be used in the models. Therefore this report aims to deliver formation factors that are defined in two different ways. The first is the "rock matrix formation factor", denoted by F_f^{rm} (–). This formation factor is representative for the solid rock matrix, as the traditional formation factor. The other one is the "fractured rock formation factor", denoted by F_f^{fr} (–), which represents the diffusive properties of a larger rock mass, where fractures and voids holding stagnant water are included in the porous system of the rock matrix. Further information on the definition of the two formation factors could be found in /4/.

The rock matrix formation factor is obtained from rock matrix resistivity data. When obtaining the rock matrix resistivity log from the in situ measurements, all resistivity data that may have been affected by open fractures have to be sorted out. With present methods one cannot with certainty separate open fractures with a significant aperture from open fractures with an insignificant aperture in the interpretation of the core logging. It should be mentioned that there is an attempt to assess the fracture aperture in the interpretation of the core logging. However, this is done on a millimetre scale. Fractures may be significant even if they only have apertures some tens of micrometers.

By investigating the rock resistivity log at a fracture, one could draw conclusions concerning the fracture aperture. However, for formation factor logging by electrical methods this is not an independent method and cannot be used. Therefore, all broken fractures have to be considered as potentially open and all resistivities obtained close to a broken fracture detected in the core logging are sorted out. By examining the resistivity logs obtained by the Century 9072 tool, it has been found that resistivity values obtained within 0.5 m from a broken fracture generally should be sorted out. This distance includes a safety margin of 0.1–0.2 m.

The fractured rock formation factor is obtained from fractured rock resistivity data. When obtaining the fractured rock resistivity log from the in situ measurements, all resistivity data that may have been affected by free water in hydraulically conductive fractures, detected in the in situ flow logging, have to be sorted out. By examining the resistivity logs obtained by the Century 9072 tool, it has been found that resistivity values obtained within 0.5 m from a hydraulically conductive fracture generally should be sorted out. This distance includes a safety margin of 0.1–0.2 m.

4.2 Rock resistivity measurements in situ

4.2.1 Rock resistivity log KFM07A

The rock resistivity of KFM07A was logged on the date 2005-02-08 (activity id 13063944) /1/. The in situ rock resistivity was obtained using the focused rock resistivity tool Century 9072. In situ rock resistivities, used in this present report, were obtained between the borehole lengths 102–993 m. In order to obtain an exact depth calibration, the track marks made in the borehole were used. According to /1/ an accurate depth calibration was obtained.

4.2.2 Rock matrix resistivity log KFM07A

All resistivity data obtained within 0.5 m from a broken fracture, detected in the core log, were sorted out from the in situ rock resistivity log. In the core log (activity id 13065700), a total of 1,143 broken fractures are recorded between 102–999 m. Ten crush zones and three zones where the core has been lost were recorded. A total of 2.3 m of the core was crushed or lost. Broken fractures can potentially intersect the borehole in zones where the core is crushed or lost. Therefore, a broken fracture was assumed every decimetre in these zones. The locations of broken fractures in KFM07A are shown in Appendix A1. A total of 4,587 rock matrix resistivities were obtained between 102–993 m. All of the rock matrix resistivity values were within the quantitative measuring range of the Century 9072 tool. The rock matrix resistivity log between 102–993 m is shown in Appendix A1.

Figure 4-2 shows the distribution of the rock matrix resistivities obtained between 102–993 m in KFM07A. The histogram ranges from 0–100,000 Ωm and is divided into sections of 5,000 Ωm.

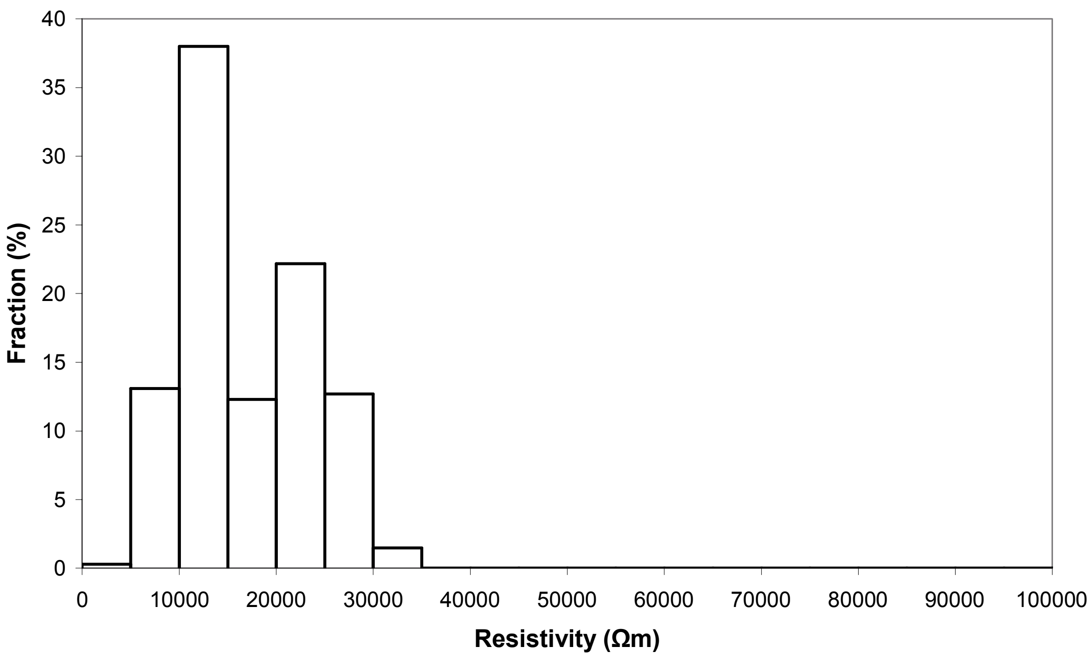

Figure 4-2. *Distribution of rock matrix resistivities in KFM07A.*

4.2.3 Fractured rock resistivity log KFM07A

All resistivity data obtained within 0.5 m from a hydraulically conductive fracture, detected in the difference flow logging /2/, were sorted out from the in situ rock resistivity log. For the difference flow log, no correction in the reported borehole length was needed. A total of 26 hydraulically conductive fractures were detected in KFM07A between 92–995 m. The locations of hydraulically conductive fractures in KFM07A are shown in Appendix A1. A total of 8,696 fractured rock resistivities were obtained between 102–993 m. All of the fractured rock resistivity values were within the quantitative measuring range of the Century 9072 tool. The fractured rock resistivity log between 102–993 m is shown in Appendix A1.

Figure 4-3 shows a histogram of the fractured rock resistivities values obtained between 102–993 m in KFM07A. The histogram ranges from 0–100,000 Ωm and is divided into sections of 5,000 Ωm.

4.2.4 Rock resistivity KFM08A

The rock resistivity of KFM08A was logged on the date 2005-04-29 (activity id 13071757) /1/. The in situ rock resistivity was obtained using the focused Century 9072 tool. In situ rock resistivities, used in this present report, were obtained between the borehole lengths 104–994 m. In order to obtain an exact depth calibration, the track marks made in the borehole were used. According to /1/ an accurate depth calibration was obtained.

4.2.5 Rock matrix resistivity log KFM08A

All resistivity data obtained within 0.5 m from a broken fracture, detected in the core log, were sorted out from the in situ rock resistivity log. In the core log (activity id 13083977), a total of 1,338 broken fractures are recorded between 102–950 m. In addition three crush zones but no zones where the core is lost are recorded. A total of 0.48 m of the core is crushed. Broken fractures can potentially intersect the borehole in zones where the core is crushed or lost. Therefore,

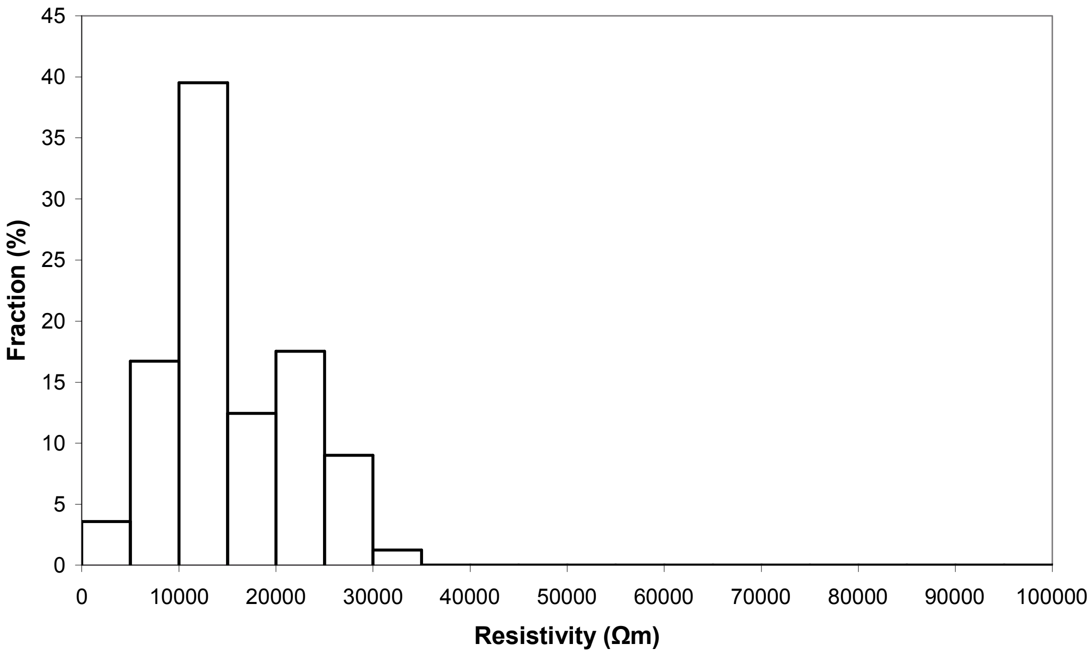

Figure 4-3. *Histogram of fractured rock resistivities in KFM07A.*

a broken fracture was assumed every decimetre in these zones. The locations of broken fractures in KFM08A are shown in Appendix A2. A total of 3,020 rock matrix resistivities were obtained between 104–950 m. 2,523 (84%) of the rock matrix resistivities were within the quantitative measuring range of the Century 9072 tool. The rock matrix resistivity log between 104–950 m is shown in Appendix A2.

Figure 4-4 shows a histogram of the rock matrix resistivities obtained between 104–950 m in KFM08A. The histogram ranges from 0–100,000 Ωm and is divided into sections of 5,000 Ωm.

4.2.6 Fractured rock resistivity log KFM08A

All resistivity data obtained within 0.5 m from a hydraulically conductive fracture, detected in the difference flow logging /3/, were sorted out from the in situ rock resistivity log. For the difference flow log, no correction in the reported borehole length was needed. A total of 41 hydraulically conductive fractures were detected in KFM08A between 94–920 m. The locations of hydraulically conductive fractures in KFM08A are shown in Appendix A2. A total of 7,754 fractured rock resistivities were obtained between 104–920 m. 6,645 (86%) of the fractured rock resistivities were within the quantitative measuring range of the Century 9072 tool. The fractured rock resistivity log between 104–920 m is shown in Appendix A2.

Figure 4-5 shows a histogram of the fractured rock resistivities obtained between 104–920 m in KFM08A. The histogram ranges from 0–100,000 Ωm and is divided into sections of 5,000 Ωm.

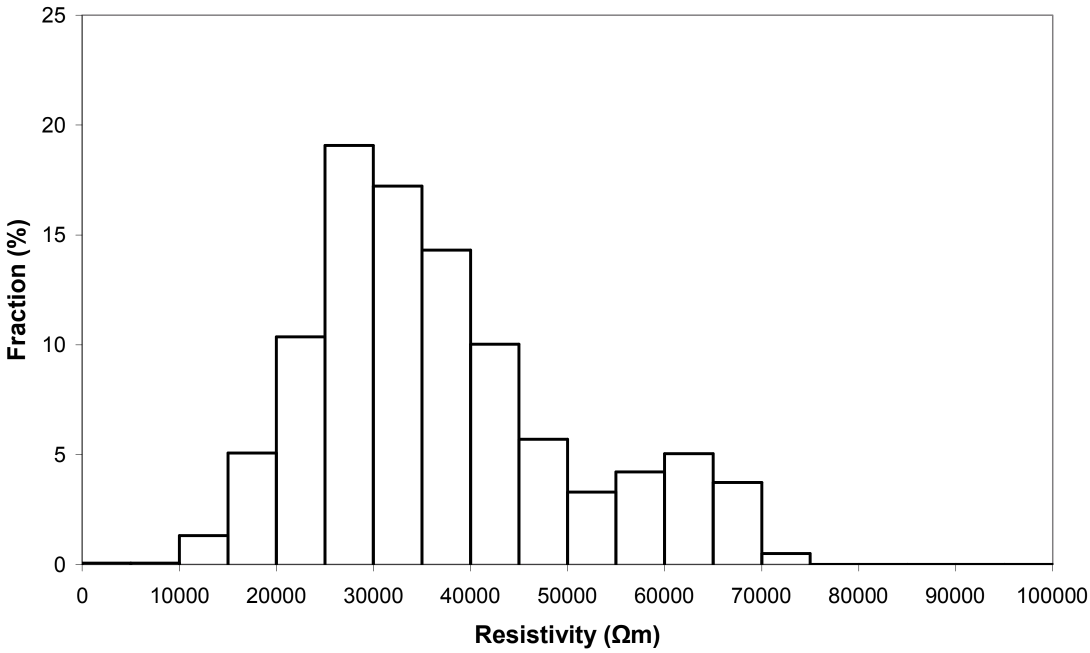

Figure 4-4. *Histogram of rock matrix resistivities in KFM08A.*

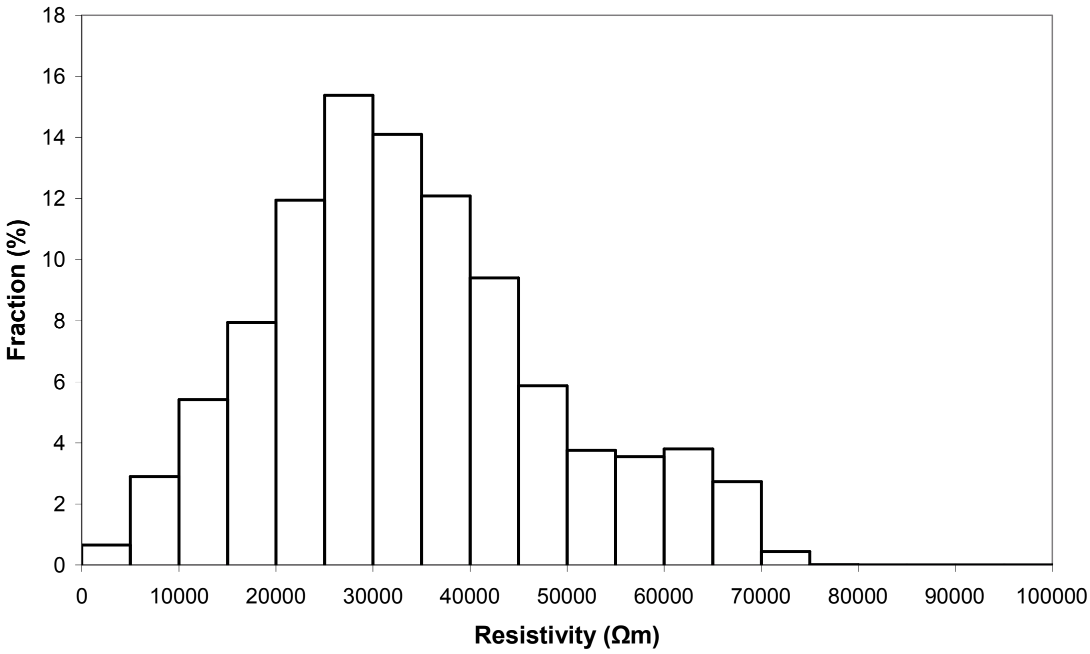

Figure 4-5. *Histogram of fractured rock resistivities in KFM08A.*

4.3 Groundwater EC measurements in situ

4.3.1 General comments

In background reports concerning the EC of the groundwater, some data have been corrected for temperature, so that they correspond to data at 25°C. Other EC data are uncorrected. Data that correspond to the temperature in situ should be used in in situ evaluations. Even though these corrections are small in comparison to the natural variation of the formation factor, measures have been taken to use data that correspond to the in situ temperature. Such data can be found in /16/.

4.3.2 EC measurements in KFM07A

The EC of the borehole fluid in KFM07A was measured before and after performing extensive pumping on the dates 2005-01-19 and 2005-01-27, respectively /2/. The lines in Figure 4-6 represent the borehole fluid EC logs obtained before (blue) and after (green) performing extensive pumping.

One can suspect that pumping had been performed prior to the campaign, as it seems that saline water had already been brought up to the 400 m level. By performing even more pumping within the campaign, saline water was brought up to the 250 m level. Hydraulically conductive fractures below 262 m are found at the borehole lengths 916.3 m, 917.2 m, and 970 m. Below 970 m, no fractures were found and the EC of the borehole fluid decreases. It is reasonable to assume that this is an artefact of the drilling and that the lower end of the borehole is filled with drilling fluid. Furthermore, it is reasonable to assume that the borehole fluid EC directly above 970 m is representative for the fracture specific EC at 970 m.

The EC of groundwater extracted from the three specific fractures at 133.7 m, 178.5 m and 261.4 m was measured by using the POSIVA difference flow meter /2/. The measurements were carried out between the dates 2005-01-25 and 2005-01-27. The transient fracture specific EC curve from 133.7 m shows a constant EC during the time measured. According to /4/ there are

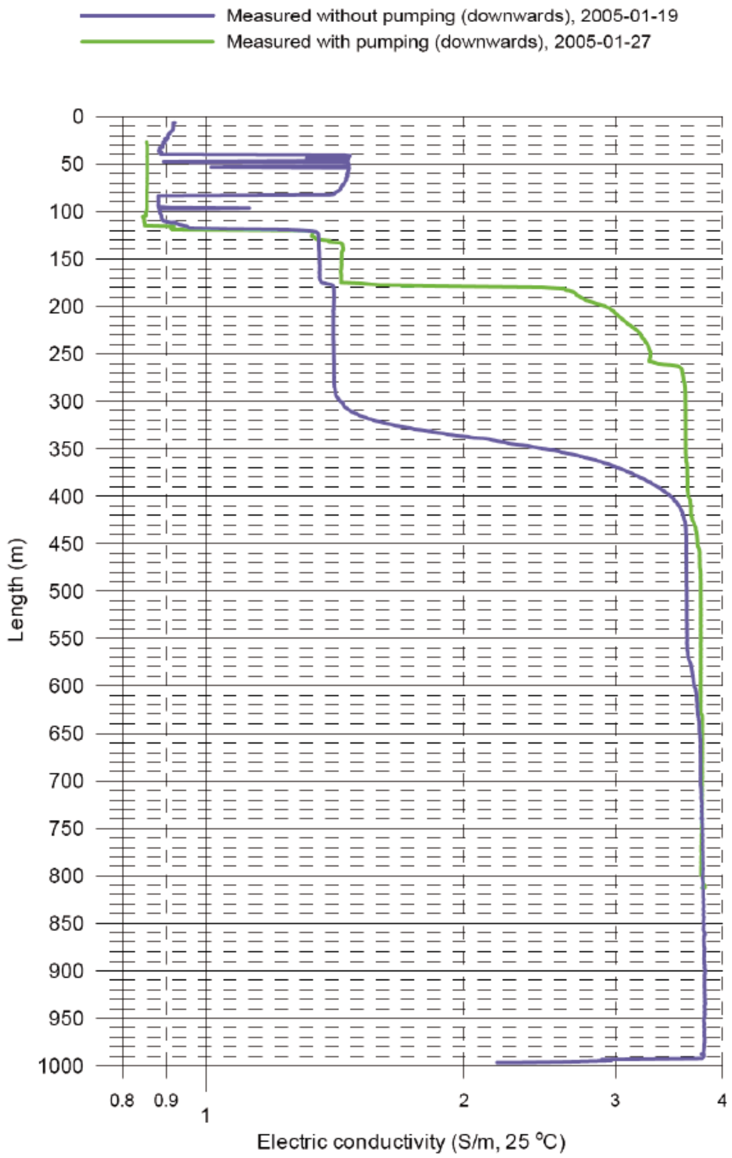

Figure 4-6. *Borehole fluid EC logs in KFM07A. Image taken from /2/.*

reasons to suspect that borehole fluid has leaked into the packed off section if one obtains a constant transient fracture specific EC curve. However, the obtained fracture specific EC does not correspond to the EC of the fluid in the tool section prior to the measurement /2/. Neither does it correspond to the borehole fluid EC obtained after extensive pumping /2/. Therefore, the obtained fracture specific EC is judged to be acceptable. The transient fracture specific EC curve for 178.5 m shows a constant EC during the time measured. The obtained fracture specific EC does not correspond to the EC of the fluid in the tool section prior to the measurement /2/. It is difficult to draw any conclusions from the comparison of the obtained fracture specific EC and the borehole fluid EC, obtained after extensive pumping, as there is a steep EC gradient in the borehole at the location. As the fracture at 178.5 m constitutes a major inflow zone into the borehole when pumping at ground surface, it is reasonable to assume that the borehole fluid directly above this location is heavily affected by the groundwater EC at 178.5 m. By comparing the borehole fluid EC directly above 178.5 m and the fracture specific EC, they were found to correspond well. Based on this information it is judged that the groundwater EC obtained at 178.5 m is reasonable. Based on the criteria described in /4/ the fracture specific EC obtained at 261.4 m is judged to be acceptable.

The EC of groundwater extracted from a packed off section between 848.6 m and 1,001.6 m in KFM07A was measured in the hydrochemical characterisation /5/. The hydrochemical characterisation was started on the date 2005-03-17 and carried out for about one month. The EC obtained in the lower 150 m of the borehole is judged to be representative for the borehole length 934 m, which is the mean borehole length of the three fractures, which can be approximated to have equal flows.

The obtained fracture specific ECs are shown in Table 4-1. Although the measurements were found acceptable, it should be noted that the representativeness of the groundwater measured on, at a specific depth, should be discussed.

4.3.3 EC measurements in KFM08A

The EC of the borehole fluid in KFM08A was measured before and after extensive pumping in a difference flow logging campaign on the dates 2005-05-13 and 2005-05-20, respectively /3/. The lines in Figure 4-6 represent the borehole fluid EC logs obtained before (turquoise) and after (green) performing extensive pumping.

The EC of groundwater extracted from a number of specific fractures between 189 m–687 m was measured in a campaign using the POSIVA difference flow meter /3/. The measurements were carried out between the dates 2005-05-18 and 2005-05-20. The resulting fracture specific ECs are shown in Table 4-2 and as black crosses in Figure 4-7. After inspecting the transient fracture specific EC curves (purple in Figure 4-7), all measurements are judged as acceptable. Although the measurements were found acceptable, it should be noted that the representativeness of the groundwater measured on, at a specific depth, should be discussed. When performing flow loggings, no hydraulically conductive fractures could be found below the borehole length 687 m /3/.

Table 4-1. Fracture specific ECs, KFM07A.

Measurment	Borehole section (m)	Location of fractures (m)	EC in situ (S/m)	EC 25°C (S/m)
Difference flow	133.24–134.24	133.7	0.79	1.19
Difference flow	178.11–179.11	178.5	0.96	1.44
Difference flow	260.86–261.86	261.4	1.81	2.65
Difference flow	Directly above 970	970.0	3.1	3.7
Hydrochemical characterisation	848.0–1,001.6	916.3, 917.2, 970.0	3.0*	3.63

*Obtained by using temperature correction based on /2/ and /16/ at that depth.

Table 4-2. Fracture specific ECs, KFM08A.

Measurment	Borehole section (m)	Location of fractures (m)	EC in situ (S/m)	EC 25°C (S/m)
Difference flow	189.15–190.15	189.8	0.41	0.62
Difference flow	189.85–190.85	190.5	0.41	0.62
Difference flow	274.58–275.58	275.0, 275.2	0.58	0.86
Difference flow	480.29–481.29	480.5	0.77	1.09
Difference flow	686.50–687.50	687.0	1.00	1.34

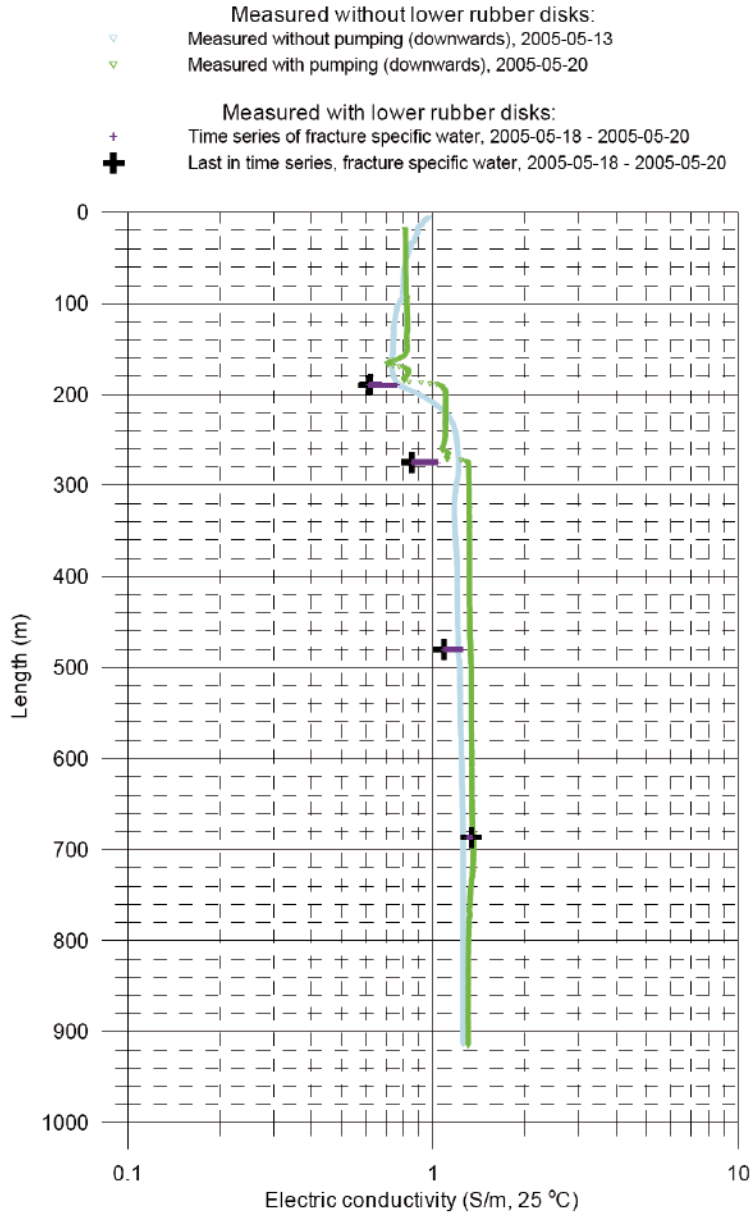

Figure 4-7. *Borehole fluid EC logs in KFM08A. Image taken from /3/.*

4.3.4 EC measurements in KFM01A–KFM08A

In KFM07A, fracture specific groundwater ECs were obtained down to the lower end of the borehole. However, there is an information gap in the borehole section 300–900 m. In KFM08A, fracture specific groundwater ECs were obtained down to a borehole length of 687 m. In order to obtain groundwater EC profiles in the boreholes, especially in the parts where there is a lack of information, fracture specific ECs from difference flow measurements and hydrochemical characterisations in the boreholes KFM01A–KMF08A were used. Fracture specific ECs in KFM01A–KFM06A are discussed in /12/.

As the boreholes have different inclinations, this was corrected for and the x-axis in Figure 4-8 represents the vertical borehole depth. When doing this correction, it was assumed that the boreholes are straight with the inclination measured at ground surface. This is not entirely true as the boreholes may be curved. Different altitudes of the drilling sites were not corrected for. In Figure 4-8 the EC values should correspond to the in situ temperature. The values are tabulated in Appendix C.

The green and red lines shown in Figure 4-8 are the assessed EC profiles of KFM07A and KFM08A, respectively. Obtaining such profiles is a somewhat subjective operation, due to lack of data. However, the variations of groundwater EC are generally small in comparison to variations in the formation factor. The exception is in the transition from fresh-meteoric waters to brackish-marine waters in the upper 200 m of the bedrock /17/. This transition appears to have occurred above the shallowest EC measuring point in both boreholes. It is recommended not to extrapolate the obtained EC profiles to borehole lengths shallower that 134 m and 190 m for KFM07A and KFM08A, respectively. For KFM08A, it is recommended not to use the EC profile shown in Figure 4-8 in formation factor calculations at shallower depth than the borehole length 250 m, due to the criterion discussed in Section 4.1.2.

As can be seen, the ECs for KFM07A are somewhat high, while the ECs for KFM08A are somewhat low, in comparison with the whole Forsmark site. Still, the assessed EC profiles in KFM07A and KFM08A differ, on average, by less than a factor of 2.

The equations for the EC-profiles shown in Figure 4-8 are the following:

KFM07A: borehole length 134–262 m,

$$\text{EC (S/m)} = 8.29\times10^{-3} \times \text{borehole length (m)} - 0.40 \qquad \text{4-4}$$

KFM07A: borehole length 262–745 m,

$$\text{EC (S/m)} = 1.77 \qquad \text{4-5}$$

KFM07A: borehole length 745–1,000 m,

$$\text{EC (S/m)} = 6.00\times10^{-3} \times \text{borehole length (m)} - 2.70 \qquad \text{4-6}$$

KFM08A: borehole length 190–690 m,

$$\text{EC (S/m)} = 1.16\times10^{-3} \times \text{borehole length (m)} + 0.21 \qquad \text{4-7}$$

KFM08A: borehole length 690–1,000 m,

$$\text{EC (S/m)} = 4.49\times10^{-3} \times \text{borehole length (m)} - 2.09 \qquad \text{4-8}$$

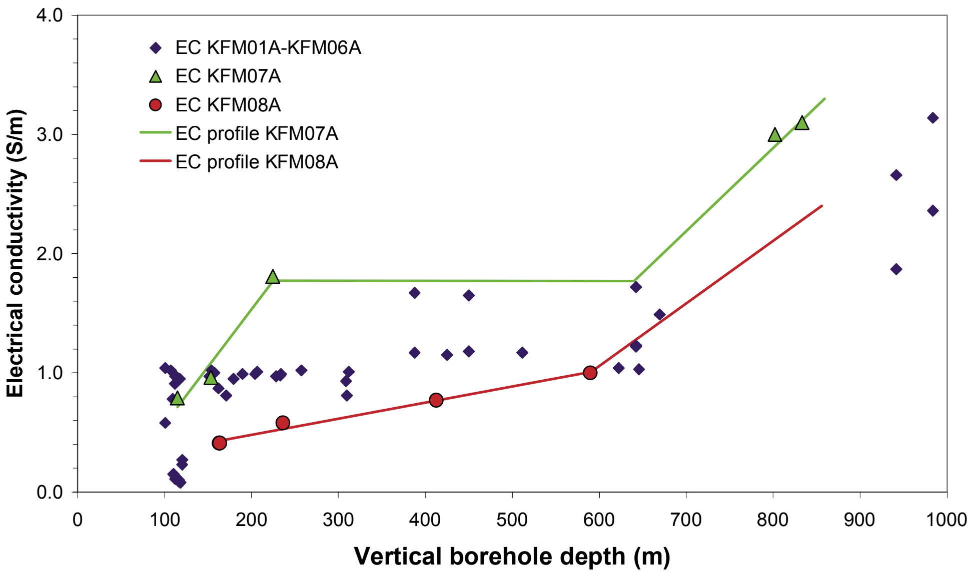

Figure 4-8. *Groundwater EC in KFM01A–KFM08A.*

4.3.5 Electrical conductivity of the pore water

In KFM07A, on average 1.3 broken fractures per metre part the drill core. From the rock resistivity log one can see that in parts of the borehole, a substantial number of the broken fractures are open with a significant aperture. In other parts of the borehole, however, this may not be the case. By visual inspection of the rock resistivity logs, shown in Appendix A1, one can see that the typical block of solid rock between open fractures with significant apertures is a few metres wide or less in the upper 300 m and the lower 200 m of the borehole. However, at many locations in the section 300–800 m the rock is very sparsely fractured. According to the measurements with the difference flow meter /2/, the upper 300 m of the borehole features a number of hydraulically conductive fractures. So does the lower 100 m. However, between 262 m and 916 m, no hydraulically conductive fractures were found. As much of the borehole features no hydraulically conductive fractures and is very sparsely fractured, the suggested EC profile is speculative.

In KFM08A, on average 1.6 broken fractures per metre part the drill core. From the rock resistivity log one can see that a substantial number of the broken fractures are open with a significant aperture. By visual inspection of the rock resistivity logs, shown in Appendix A2, one can see that the typical block of solid rock between open fractures with significant apertures is a few metres wide or less. No extensive difference in fracture frequency can be seen between the upper and lower part of the borehole. According to the measurements with the difference flow meter /3/, the upper 500 m of the borehole features numerous hydraulically conductive fractures. Below 500 m, only one hydraulically conductive fracture was found (at 687 m). As the lower 500 m of the borehole features practically no hydraulically conductive fractures, the suggested EC profile is somewhat speculative.

In KFM07A, and KFM08A, and probably to some extent in all boreholes with conductive fractures at depth at the site, there is a risk that saline water from a greater depth has been brought to shallower depth when performing pumping. This saline groundwater may affect the obtained fracture specific ECs. Generally one should also take into account that the borehole itself functions as a hydraulical conductor, enabling groundwater to be quickly transported from one depth to another. Such considerations are made in /18/ for the Laxemar site. It appears, however, that the groundwater EC is less affected by such effects in Forsmark than in Laxemar. As can be seen from Figure 4-8, the EC data obtained at repository depth and surroundings (300–700 m) at the Forsmark site only varies by about a factor of two.

4.4 Formation factor measurements in the laboratory

Formation factors have not been estimated in the laboratory for KFM07A and KFM08A.

4.5 Nonconformities

The work was carried out in accordance with the activity plan and the method description without nonconformities. However, the limited quantitative measuring range of the in situ rock resistivity tool may give rise to overestimations of formation factors in the lower formation factor range in KFM08A.

5 Results

5.1 In situ rock matrix formation factor

The in situ formation factors obtained in KFM07A and KFM08A were treated statistically. By using the normal-score method, as described in /19/, to determine the likelihood that a set of data is normally distributed, the mean value and standard deviation of the logarithm ($\log_{10}$) of the formation factors could be determined. Figure 5-1 shows the distributions of the rock matrix formation factors obtained in situ between 134–993 m in KFM07A and between 250–950 m in KFM08A.

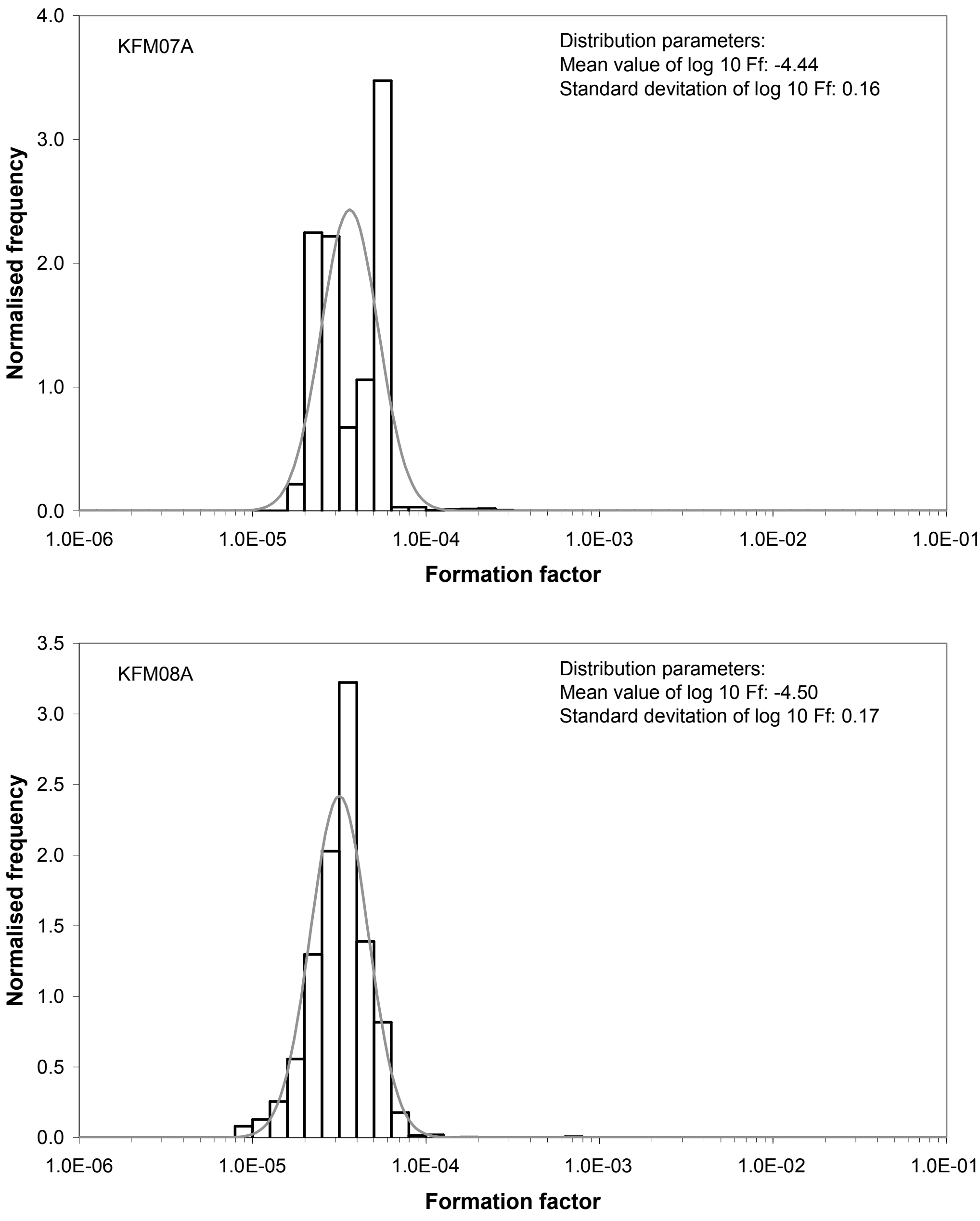

Figure 5-1. *Distributions of in situ rock matrix formation factors in KFM07A and KFM08A.*

The rock matrix formation factor distribution of KFM07A shows dual peaks. If examining the rock resistivity log of KFM07A, shown in Figure 5-2, one can see a pronounced resistivity gradient between 500 m and 600 m.

Based on this, one could suggest, with the prerequisite that the formation factor does not vary with depth, that the transition between brackish and saline ground- and pore water is found between the borehole lengths 500 m and 600 m. Such a transition is not reflected in Figure 4-8. However, it is chosen not to alter the suggested groundwater EC profile on basis of the resulting formation factor log, as the entities are not independent. However, an errorous groundwater EC profile would, at least partly, explain the dual peaks in of the rock matrix formation factor distribution for KFM07A.

The rock matrix formation factors of KFM08A appear to be log-normally distributed. The mean values and standard deviations of the distributions in Figure 5-1 are shown in Table 5-1 and Table 5-2 for KFM07A and KFM08A, respectively. The in situ rock matrix formation factor logs of KFM07A and KFM08A are shown in Appendix B1 and B2, respectively.

5.2 In situ fractured rock formation factor

Figure 5-3 shows the distributions of the fractured rock formation factors obtained in situ between 134–993 m in KFM07A and between 250–920 m in KFM08A.

The distributions strongly resemble those in Figure 5-1, except for a deviation in the upper formation factor region. Here, some of the obtained formation factors are affected by free water in hydraulically non-conductive fractures. The mean values and standard deviations of the distributions in Figure 5-3 are shown in Table 5-1 and Table 5-2 for KFM07A and KFM08A, respectively. The in situ fractured rock formation factor logs of KFM07A and KFM08A are shown in Appendix B1 and B2, respectively.

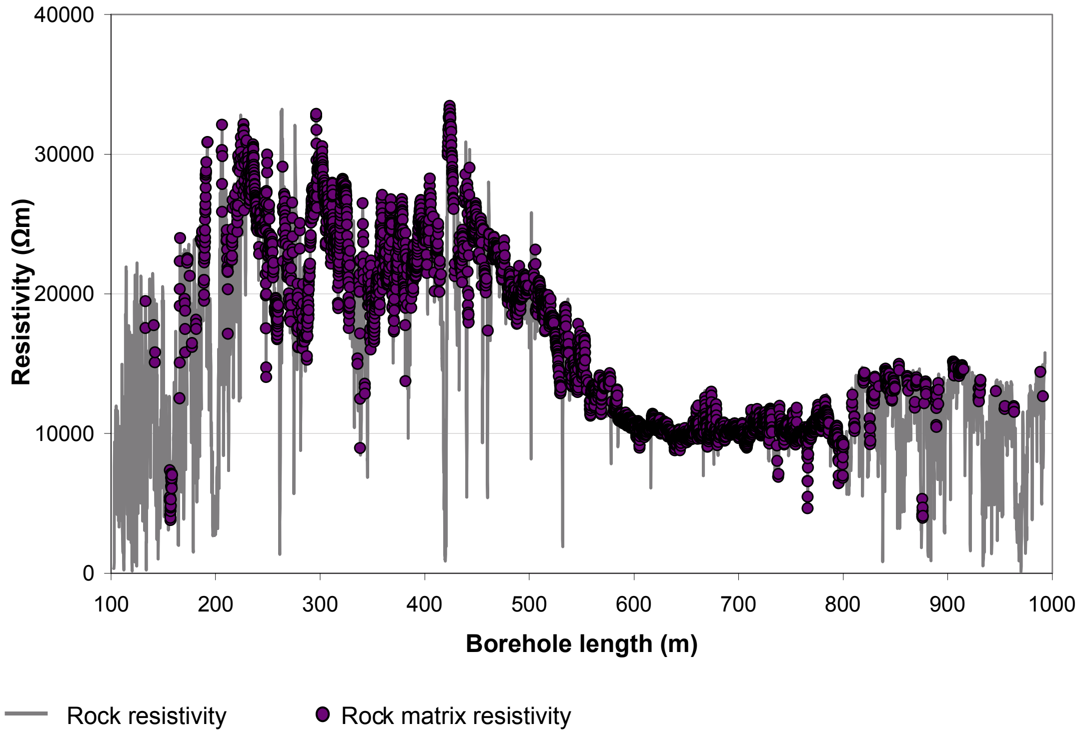

Figure 5-2. Rock matrix resistivity log of KFM07A. Shown in detail in Appendix A1.

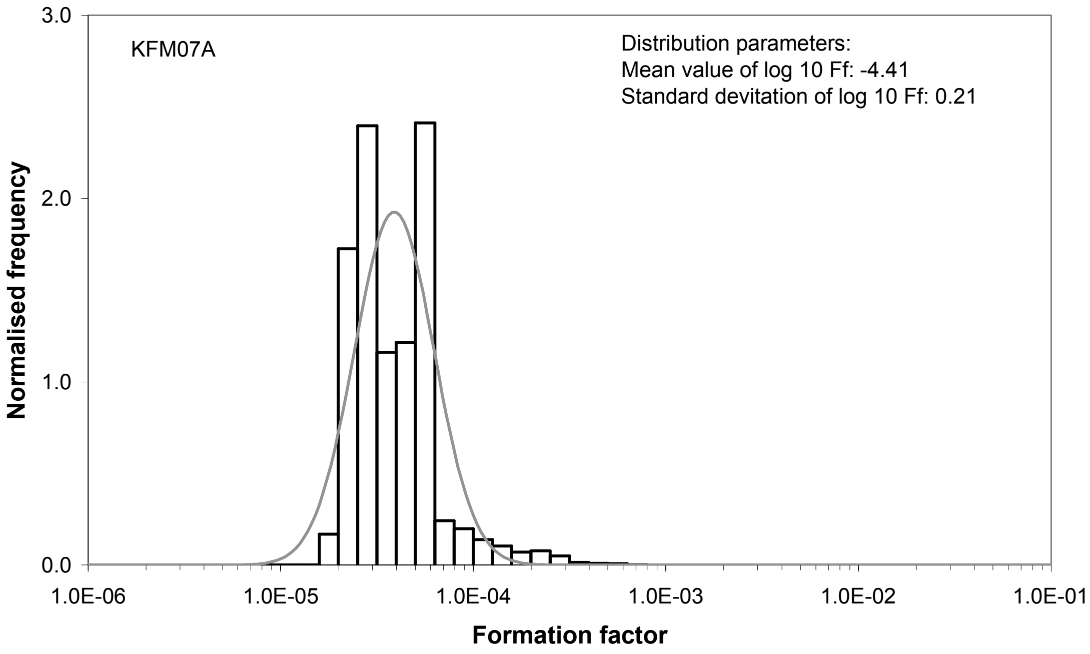

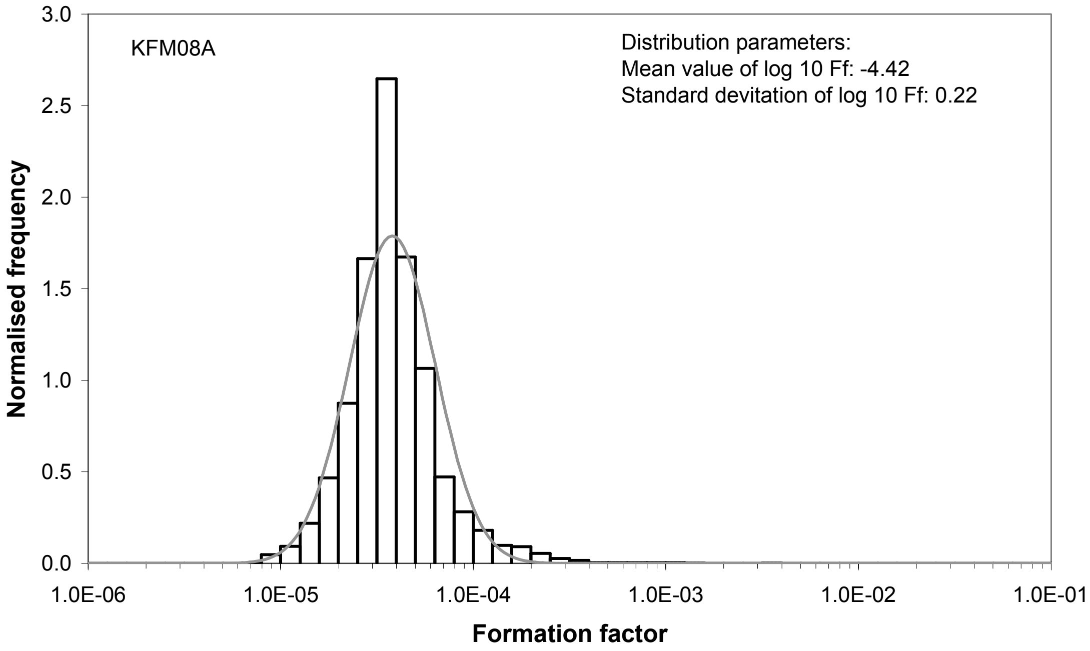

Figure 5-3. *Distributions of in situ fractured rock formation factors in KFM07A and KFM08A.*

5.3 Comparison of formation factors of KFM07A

Table 5-1 presents mean values and standard deviations of the log-normal distributions shown in Figures 5-1 and 5-3 for KFM07A. In addition, the number of data points obtained and the arithmetic mean values for the different formation factors are shown.

As seen in Table 5-1, the fractured rock formation factors are, on average, only slightly larger than the rock matrix formation factors. This is explained by the fact that much of the rock surrounding KFM07A is very sparsely fractured.

Table 5-1. Distribution parameters and arithmetic mean value of the formation factor, KFM07A.

Formation factor	Number of data points	Mean $\log_{10}(F_f)$	Standard deviation $\log_{10}(F_f)$	Arithmetic mean F_f
In situ Rock matrix F_f	4,585	–4.44	0.164	3.95×10^{-5}
In situ Fractured rock F_f	8,760	–4.41	0.207	4.63×10^{-5}

5.4 Comparison of formation factors of KFM08A

Table 5-2 presents mean values and standard deviations of the log-normal distributions shown in Figures 5-1 and 5-3 for KFM08A. In addition, the number of data points obtained and the arithmetic mean values for the different formation factors are shown.

It should be noted from Table 5-2 that the fractured rock formation factors are, on average, 1.4 times as large as the rock matrix formation factors.

Table 5-2. Distribution parameters and arithmetic mean value of the formation factor, KFM08A.

Formation factor	Number of data points	Mean $\log_{10}(F_f)$	Standard deviation $\log_{10}(F_f)$	Arithmetic mean F_f
In situ Rock matrix F_f	2,607	–4.50	0.165	3.45×10^{-5}
In situ Fractured rock F_f	7,957	–4.42	0.223	4.68×10^{-5}

6 Summary and discussions

The formation factors obtained in KFM07A and KFM08A range from 8.9×10^{-6} to 3.8×10^{-3}. The formation factors appear to be fairly well distributed according to the log-normal distribution, even though there are some deviations in data from KFM07A. The obtained in situ distributions have mean values for $\log_{10}(F_f)$ between –4.5 and –4.4 and standard deviations between 0.16 and 0.22. The arithmetic mean values range between 3.5×10^{-5} and 4.7×10^{-5}.

The fractured rock formation factors were on average only slightly larger than the rock matrix formation factors. This indicates that the retention capacity for non-sorbing species due to open, but hydraulically non-conductive, fractures is lower in the rock surrounding these boreholes. It should be noted that the rock surrounding KFM07A in large sections is very sparsely fractured. This may be of relevance for the electrical conductivity of the pore water, which appeared to be more saline at and below repository depth than at other investigated locations in the Forsmark area.

Judging from the obtained formation factor histograms, only a small fraction of the obtained in situ rock resistivities in KFM08A may have been affected by limitations of the in situ rock resistivity tool.

References

/1/ **Nielsen U T, Ringgaard J, 2005.** Geophysical borehole logging in boreholes KFM07A, KFM08A and KFM08B. Site investigation report. SKB P-04-159. Svensk Kärnbränslehantering AB.

/2/ **Sokolnicki M, Rouhiainen P, 2005.** Difference flow logging in borehole KFM07A. Site investigation report. SKB P-05-63. Svensk Kärnbränslehantering AB.

/3/ **Sokolnicki M, Rouhiainen P, 2005.** Difference flow logging in borehole KFM08A. Site investigation report. SKB P-05-43. Svensk Kärnbränslehantering AB.

/4/ **Löfgren M, Neretnieks I, 2005.** Formation factor logging in situ and in the laboratory by electrical methods in KSH01A and KSH02: Measurements and evaluation of methodology. Site investigation report. SKB P-05-27. Svensk Kärnbränslehantering AB.

/5/ **Berg C, Wacker P, Nilsson A-C, 2005.** Chemical characterisation in borehole KFM07A. Results from the investigated section at 848.0–1,001.6 m. Site investigation report. SKB P-05-170. Svensk Kärnbränslehantering AB.

/6/ **Petersson J, Skogmo G, Wängnerud A, Berglund J, Stråhle A, 2005.** Boremap mapping of telescopic drilled borehole KFM07A. Site investigation report. SKB P-05-102. Svensk Kärnbränslehantering AB.

/7/ **Petersson J, Skogsmo G, Berglund J, Wängnerud A, Danielsson P, Stråhle A, 2005.** Boremap mapping of telescopic drilled borehole KFM08A and core drilled borehole KFM08B. Site investigation report. SKB P-05-203. Svensk Kärnbränslehantering AB.

/8/ **Ehrenborg J, Stejskal V, 2004.** Boremap mapping of core drilled boreholes KSH01A and KSH01B. Site investigation report. SKB P-04-01. Svensk Kärnbränslehantering AB.

/9/ **Löfgren M, Neretnieks I, 2002.** Formation factor logging in situ by electrical methods. Background and methodology. SKB TR-02-27. Svensk Kärnbränslehantering AB.

/10/ **Löfgren M, 2001.** Formation factor logging in igneous rock by electrical methods. Licentiate thesis at the Royal Institute of Technology, Stockholm, Sweden. ISBN 91-7283-207-x.

/11/ **Waber H N, Smellie J A T, 2005.** Borehole KFM06A: Characterisation of pore water. Part 1: Diffusion experiments. Site investigation report. SKB P-05-196. Svensk Kärnbränslehantering AB.

/12/ **Löfgren M, Pettersson M, Widén H, Crawford J, 2006.** Formation factor logging in situ by electrical methods in KFM05A and KFM06A. Site Investigation Report. SKB P-06-91. Svensk Kärnbränslehantering AB.

/13/ **Ohlsson Y, 2000.** Studies of Ionic Diffusion in Crystalline Rock. Doctoral thesis at the Royal Institute of Technology, Stockholm, Sweden. ISBN 91-7283-025-5.

/14/ **Löfgren M, 2004.** Diffusive properties of granitic rock as measured by in situ electrical methods. Doctoral thesis at the Royal Institute of Technology, Stockholm, Sweden. ISBN 91-7283-935-X.

/15/ **Löfgren M, Neretnieks I, 2006.** Through-electromigration: A new method of investigating pore connectivity and obtaining formation factors. Accepted for publication in Journal of Contaminant Hydration, 2006.

/16/ **SICADA, 2006.** Site Characterisation Data Base, Svensk Kärnbränslehantering AB.

/17/ **Laaksoharju M, Gimeno M, Auqué L, Gómez J, Smellie J, Tullborg E-L, Gurban I, 2004.** Hydrogeochemical evaluation of the Forsmark site, model version 1.1. SKB R-04-05. Svensk Kärnbränslehantering AB.

/18/ **Löfgren M, Pettersson M, 2006.** Formation factor logging in situ by electrical methods in KLX05 and KLX06. Site Investigation Report. SKB P-06-146. Svensk Kärnbränslehantering AB.

/19/ **Johnson RA, 1994.** Miller and Freund's probability & statistics for engineers, 5ed. Prentice-Hall Inc., ISBN 0-13-721408-1.

Appendix A1. In situ rock resistivities and fractures KFM07A

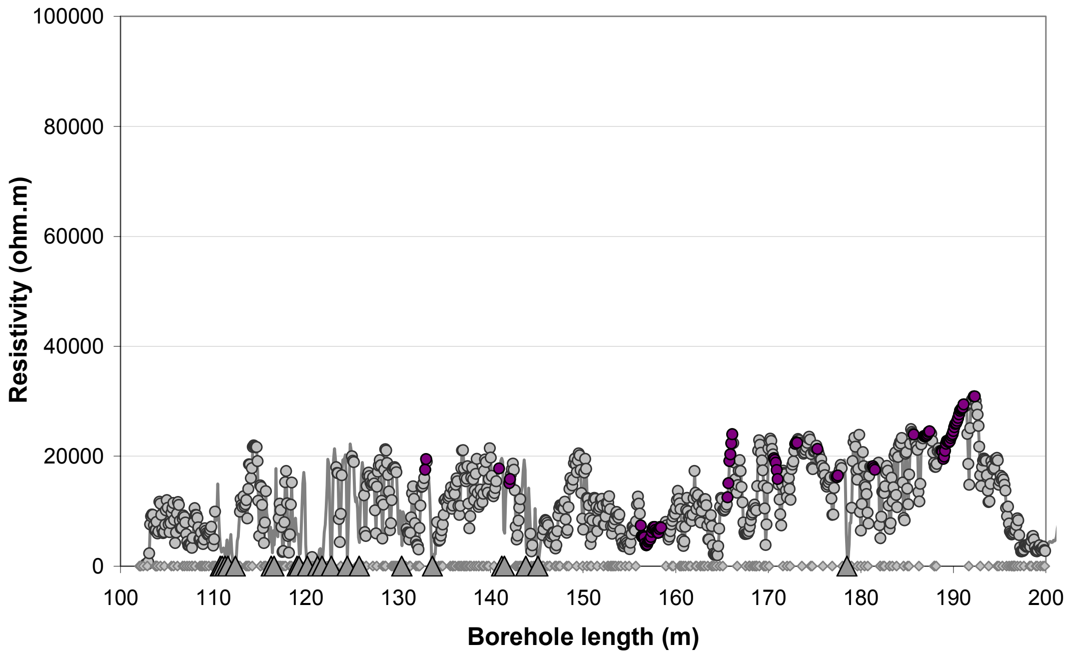

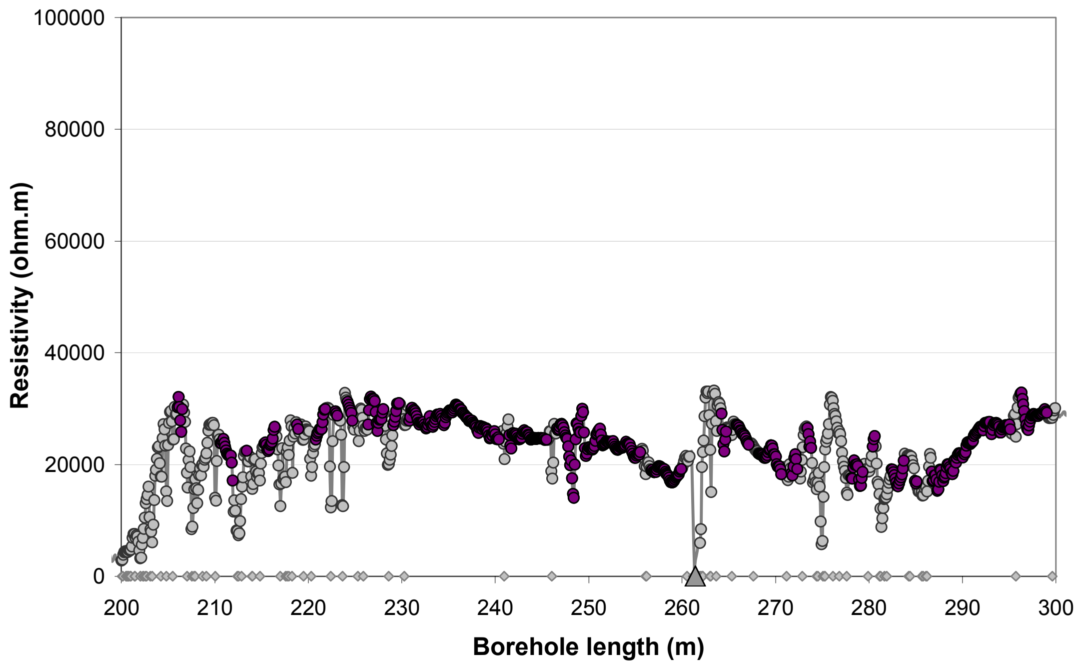

Rock resistivity
Fractured rock resistivity
Rock matrix resistivity
Location of broken fracture parting the drill core
Location of hydraulically conductive fracture detected in the difference flow logging

Appendix A1: **In-situ rock resistivities and fractures KFM07A**

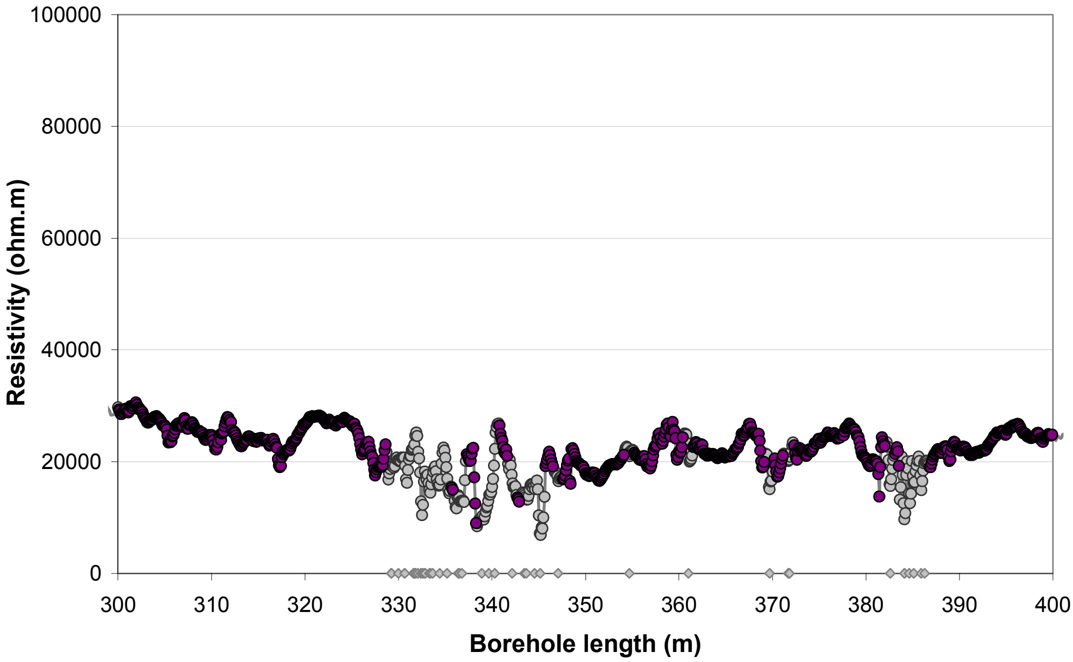

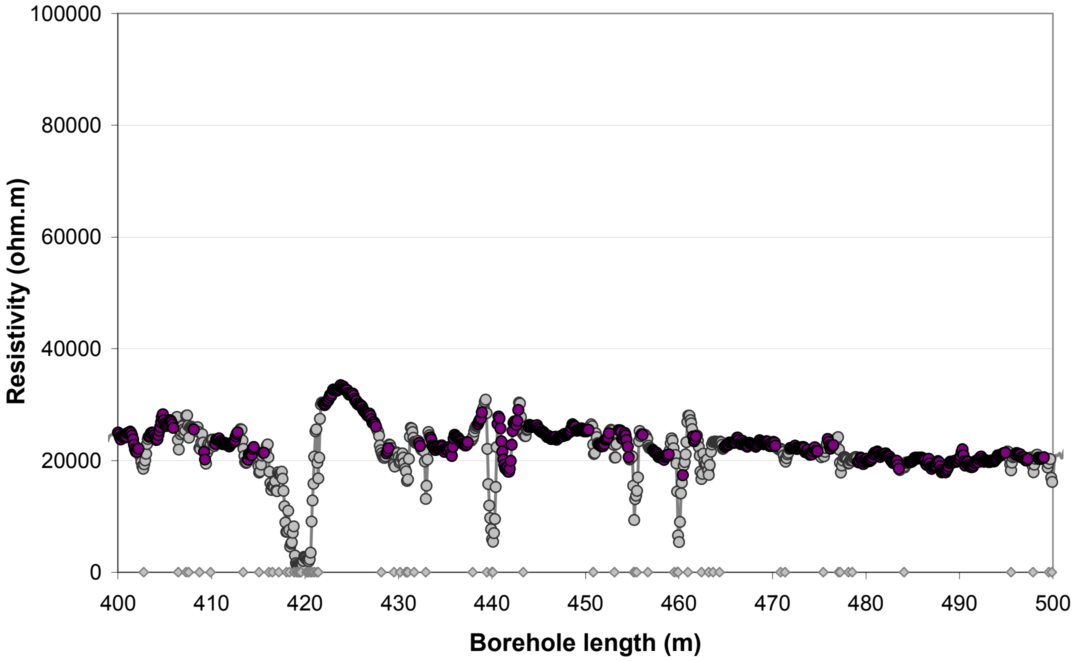

- Rock resistivity
- Fractured rock resistivity
- Rock matrix resistivity
- Location of broken fracture parting the drill core
- Location of hydraulically conductive fracture detected in the difference flow logging

Appendix A1: **In-situ rock resistivities and fractures KFM07A**

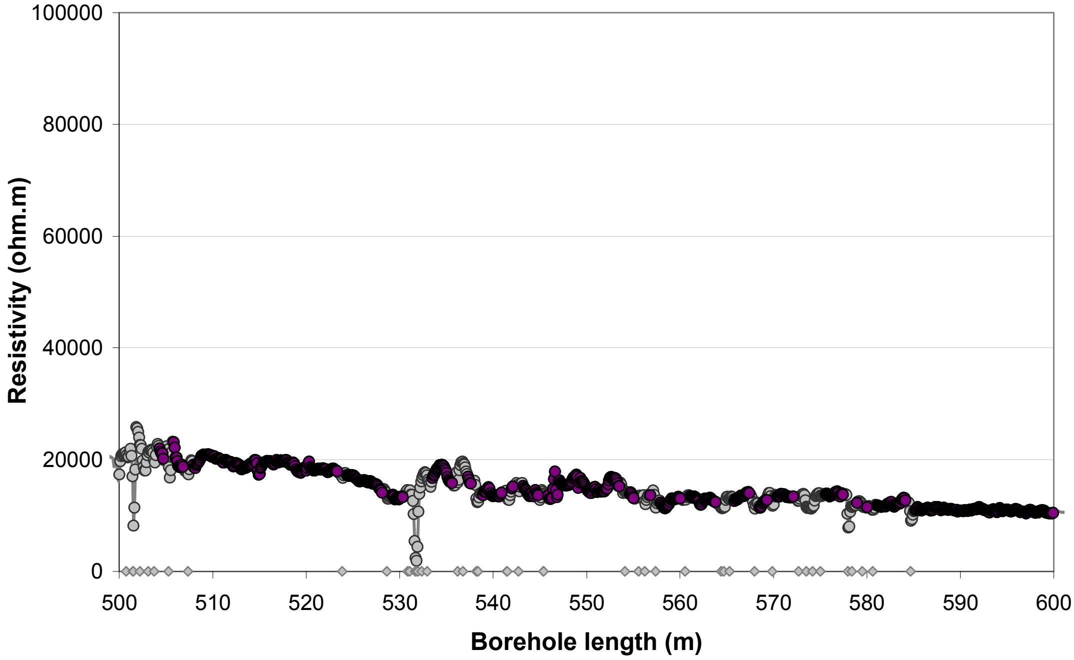

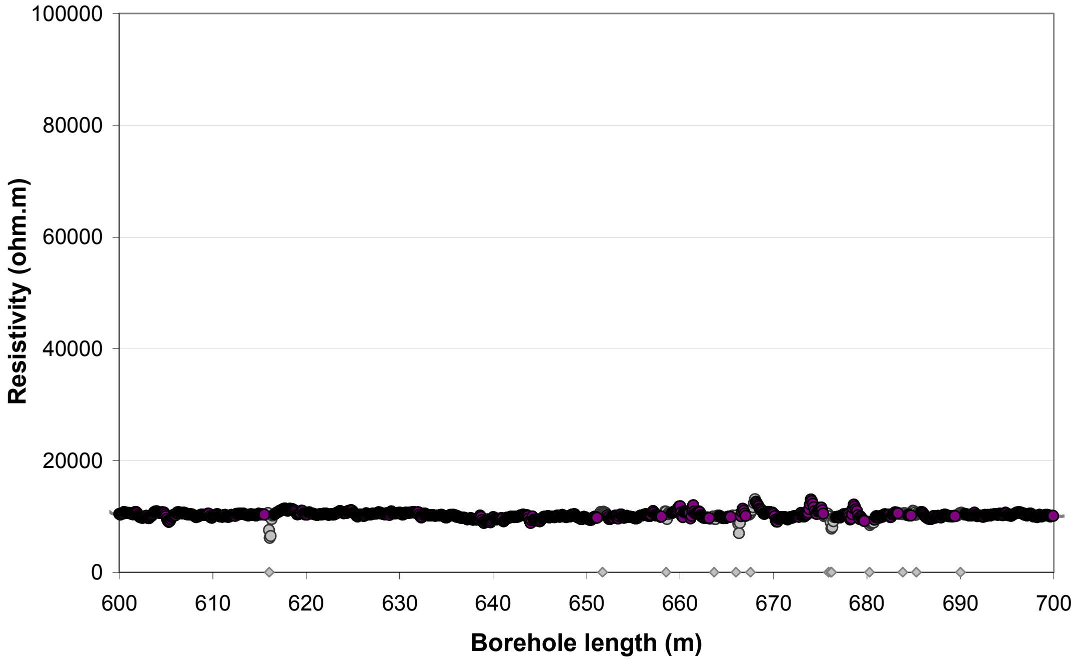

Rock resistivity
Fractured rock resistivity
Rock matrix resistivity
Location of broken fracture parting the drill core
Location of hydraulically conductive fracture detected in the difference flow logging

Appendix A1: **In-situ rock resistivities and fractures KFM07A**

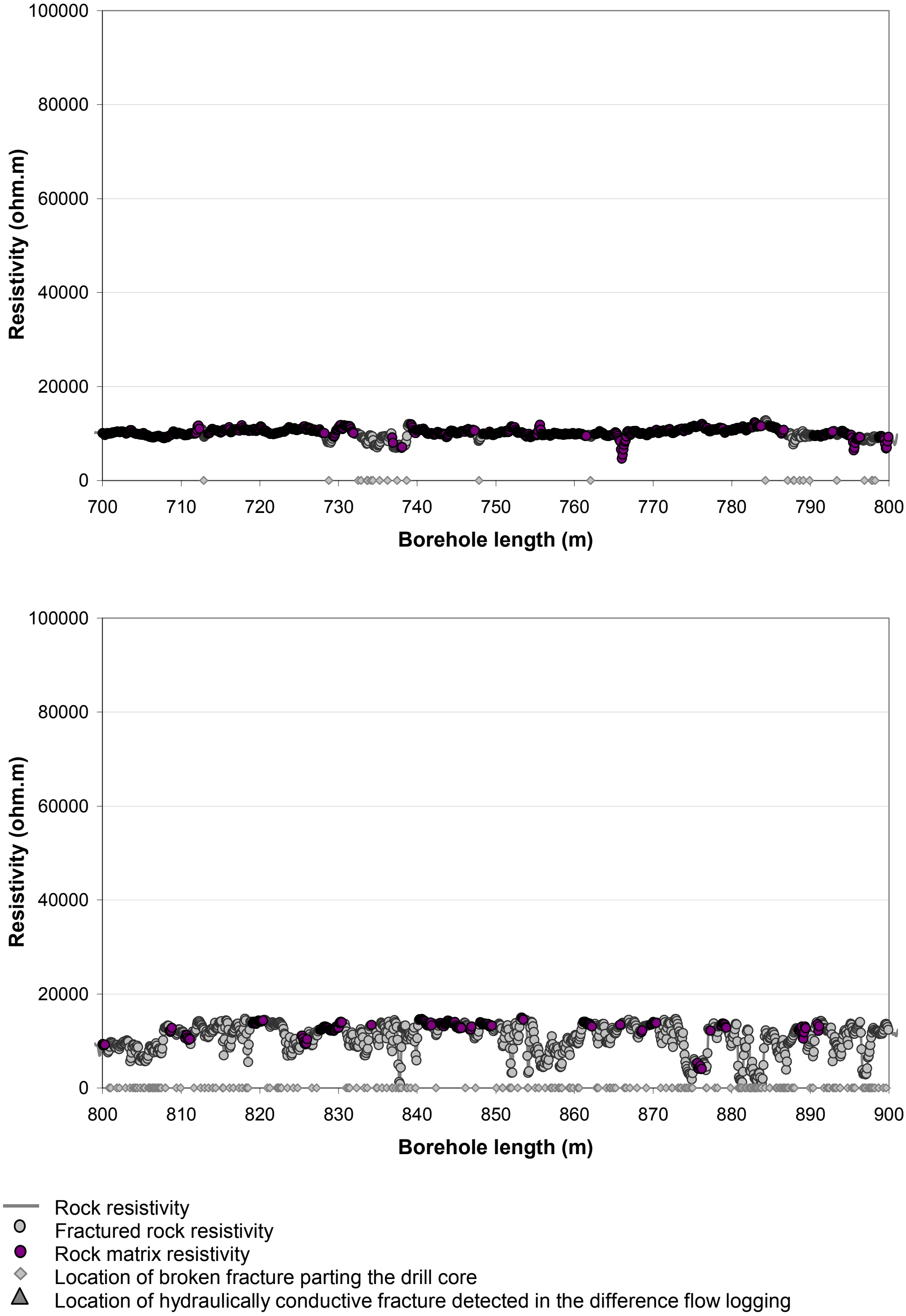

Appendix A1: **In-situ rock resistivities and fractures KFM07A**

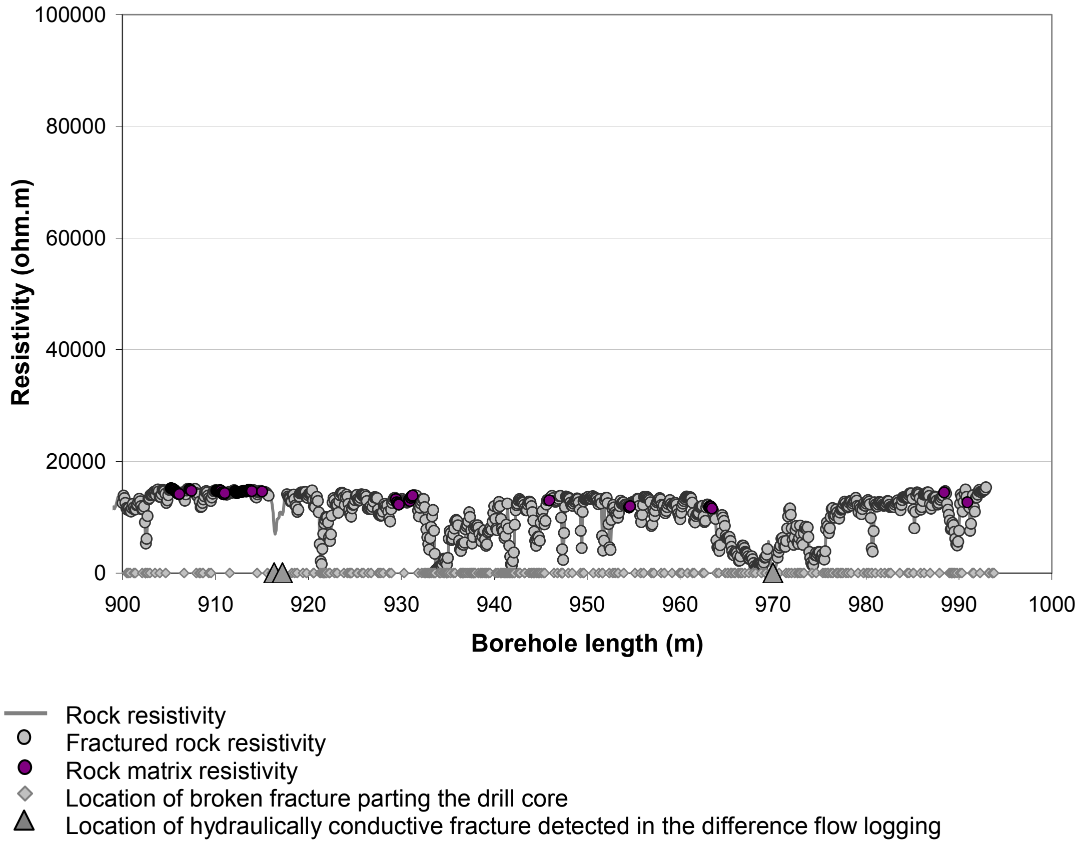

Appendix A2. In situ rock resistivities and fractures KFM08A

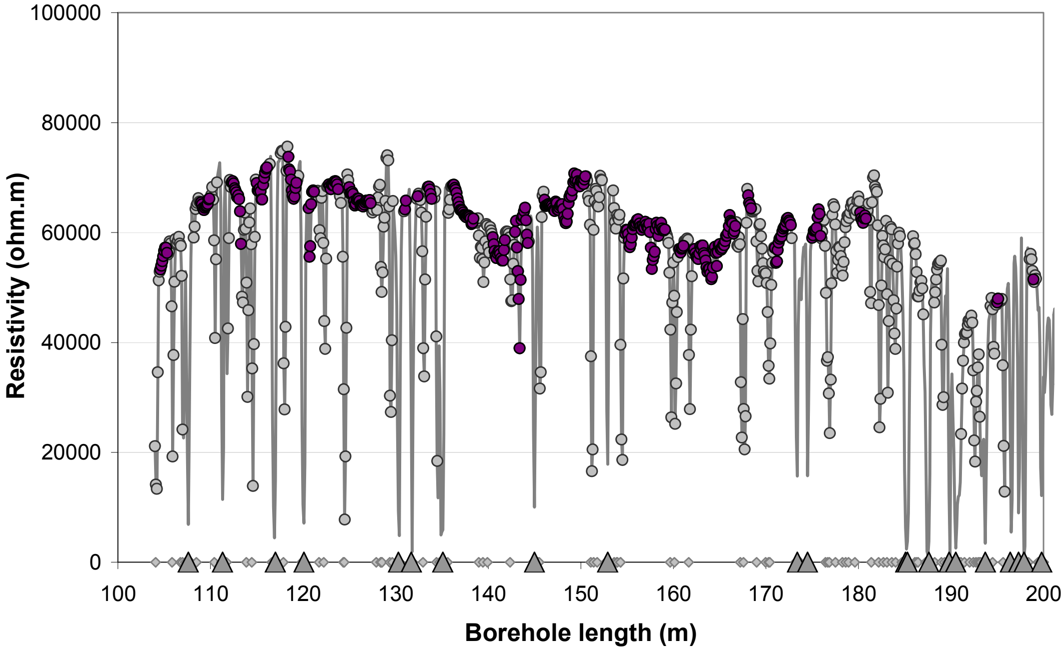

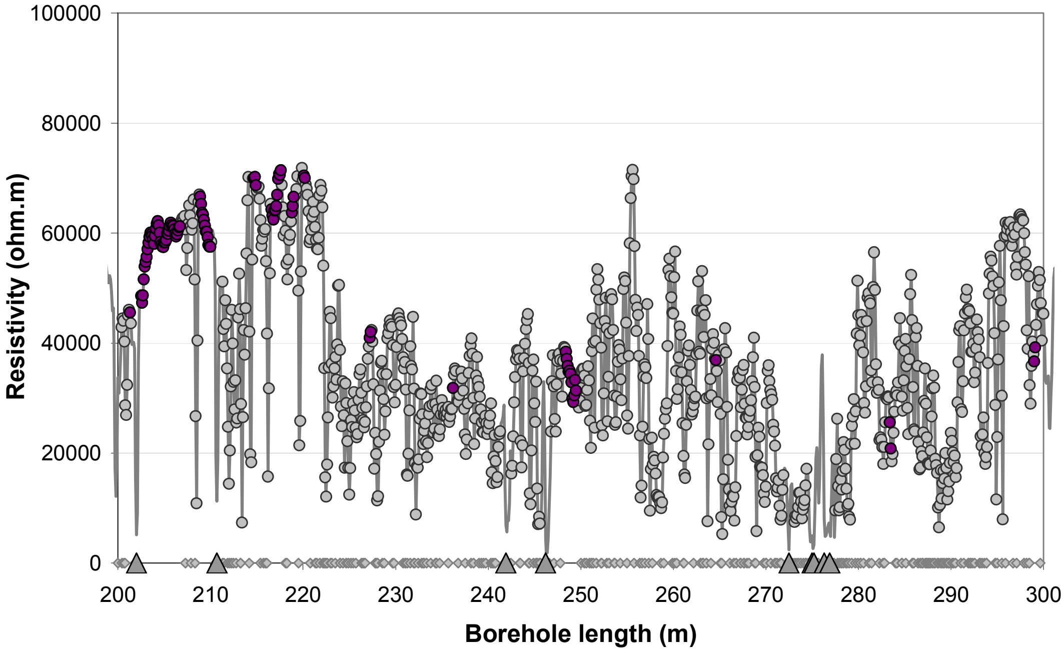

Rock resistivity
Fractured rock resistivity
Rock matrix resistivity
Location of broken fracture parting the drill core
Location of hydraulically conductive fracture detected in the difference flow logging

Appendix A2: **In-situ rock resistivities and fractures KFM08A**

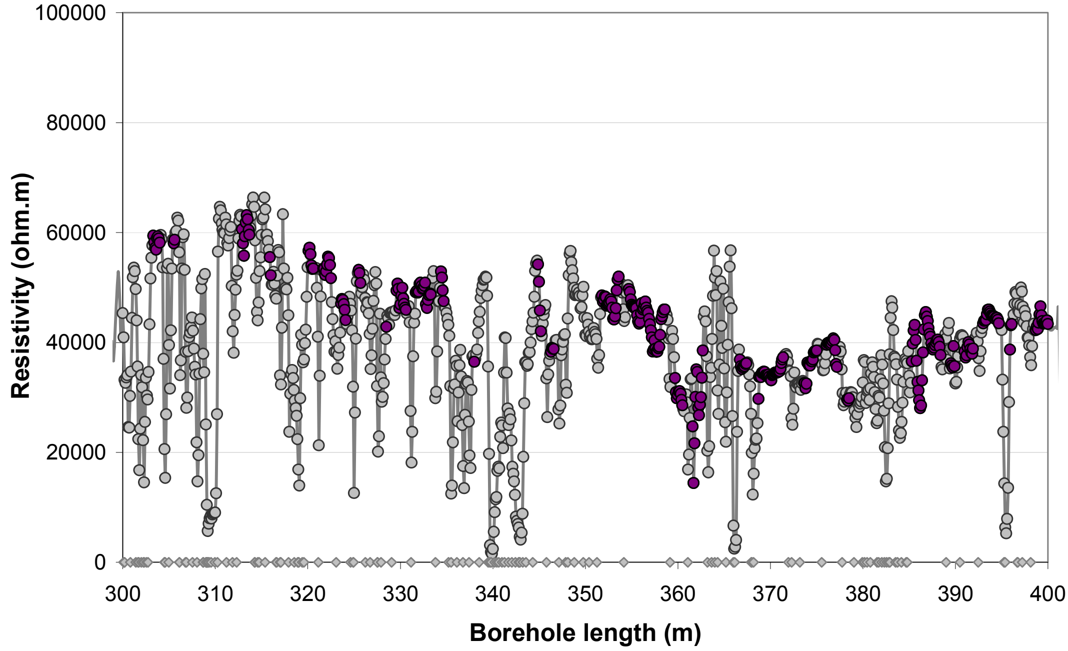

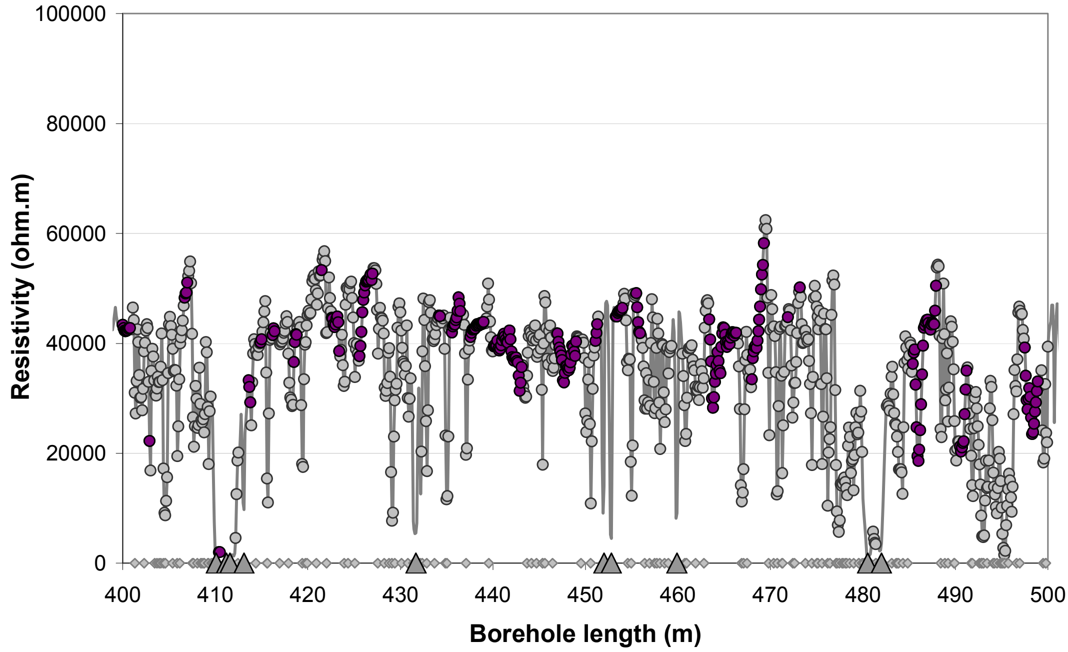

- Rock resistivity
- Fractured rock resistivity
- Rock matrix resistivity
- Location of broken fracture parting the drill core
- Location of hydraulically conductive fracture detected in the difference flow logging

Appendix A2: **In-situ rock resistivities and fractures KFM08A**

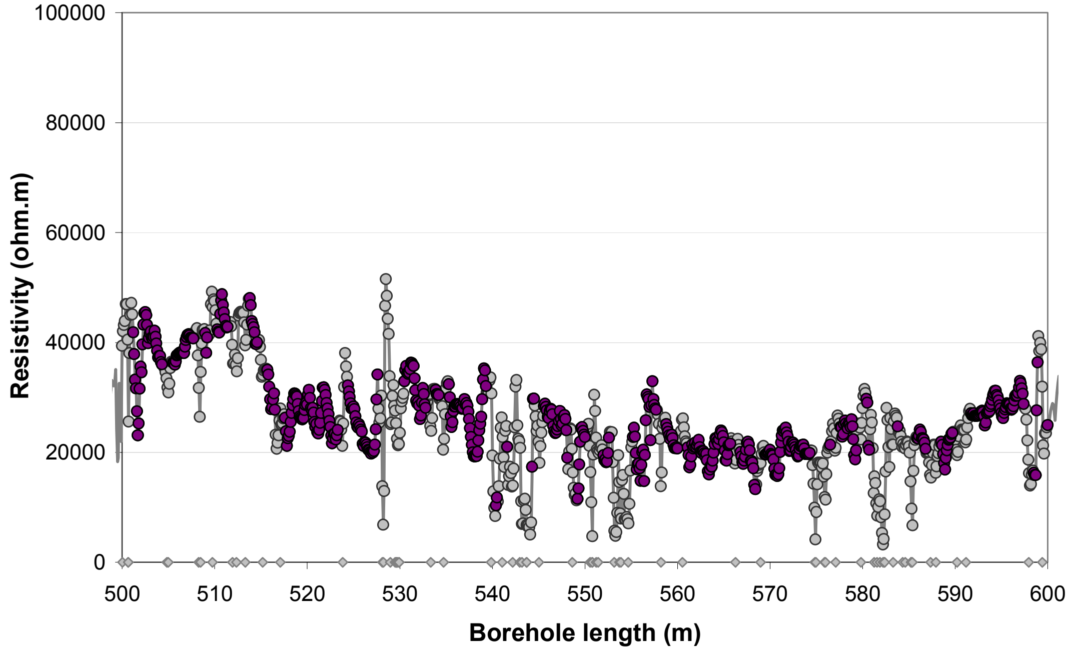

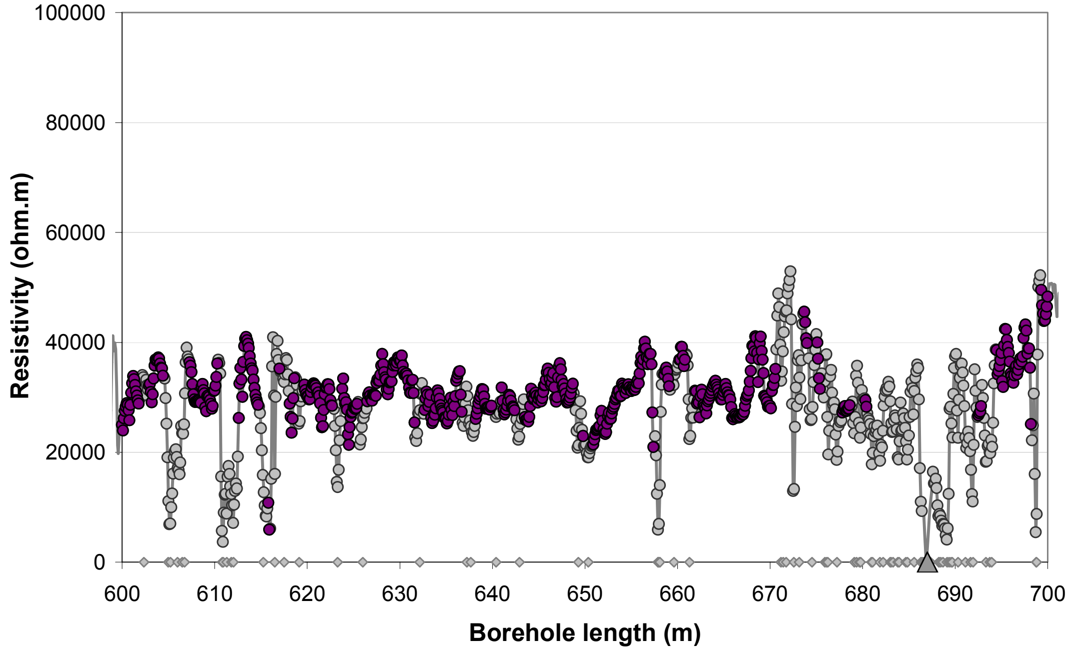

Rock resistivity
Fractured rock resistivity
Rock matrix resistivity
Location of broken fracture parting the drill core
Location of hydraulically conductive fracture detected in the difference flow logging

Appendix A2: **In-situ rock resistivities and fractures KFM08A**

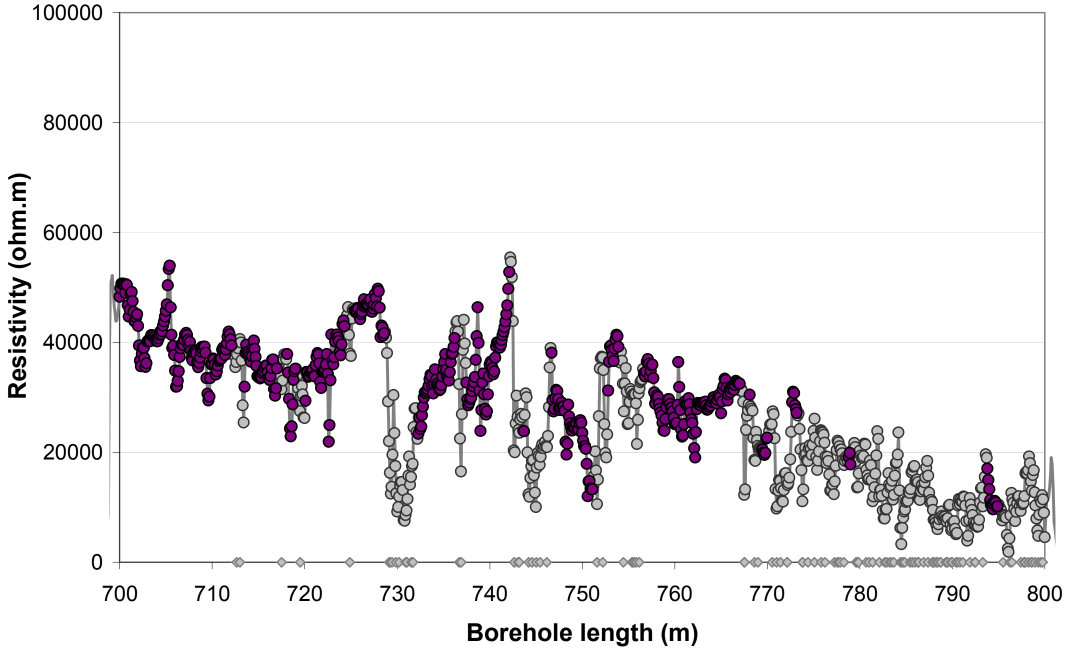

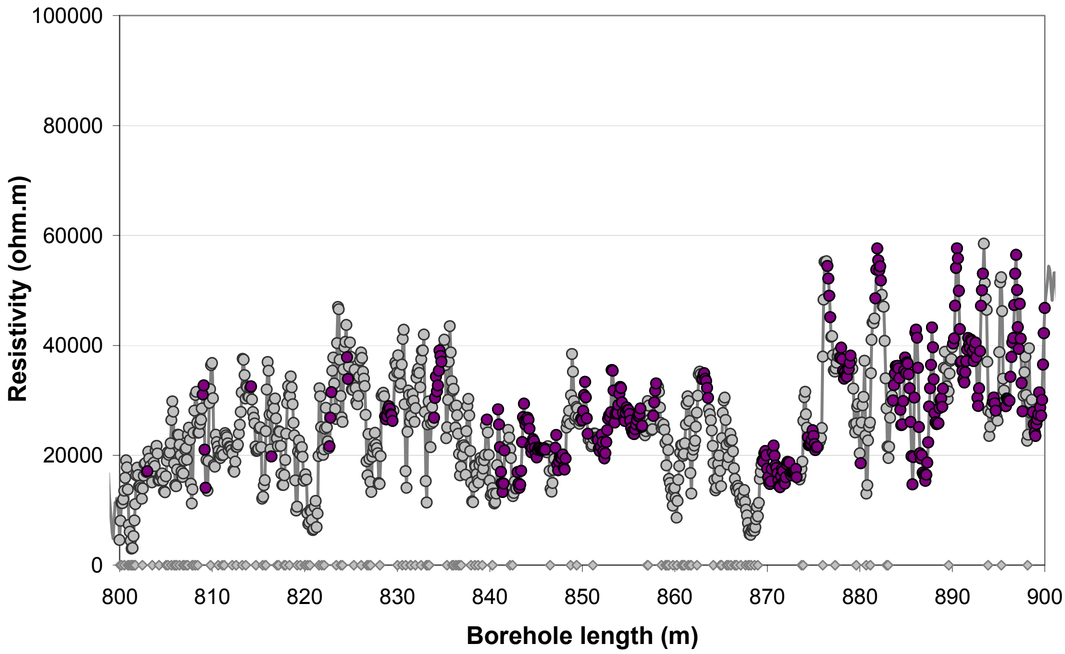

Rock resistivity
Fractured rock resistivity
Rock matrix resistivity
Location of broken fracture parting the drill core
Location of hydraulically conductive fracture detected in the difference flow logging

Appendix A2: **In-situ rock resistivities and fractures KFM08A**

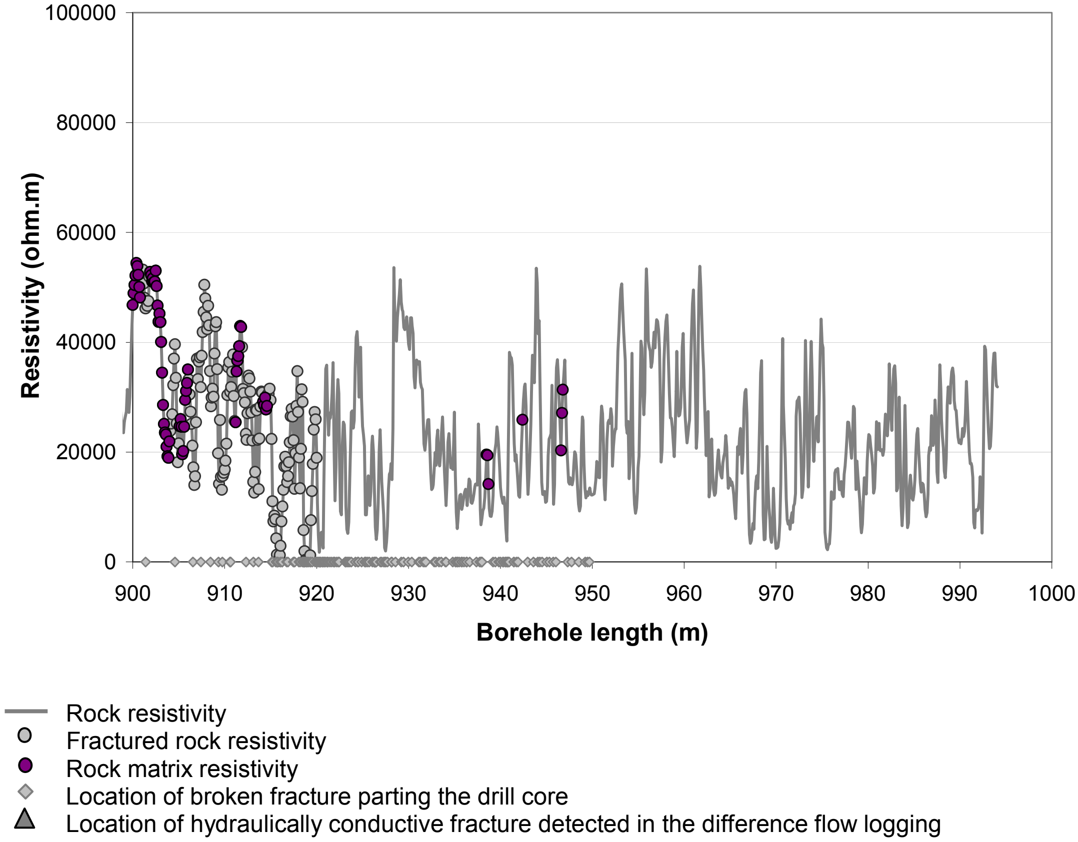

Appendix B

Appendix B1. In situ formation factors KFM07A

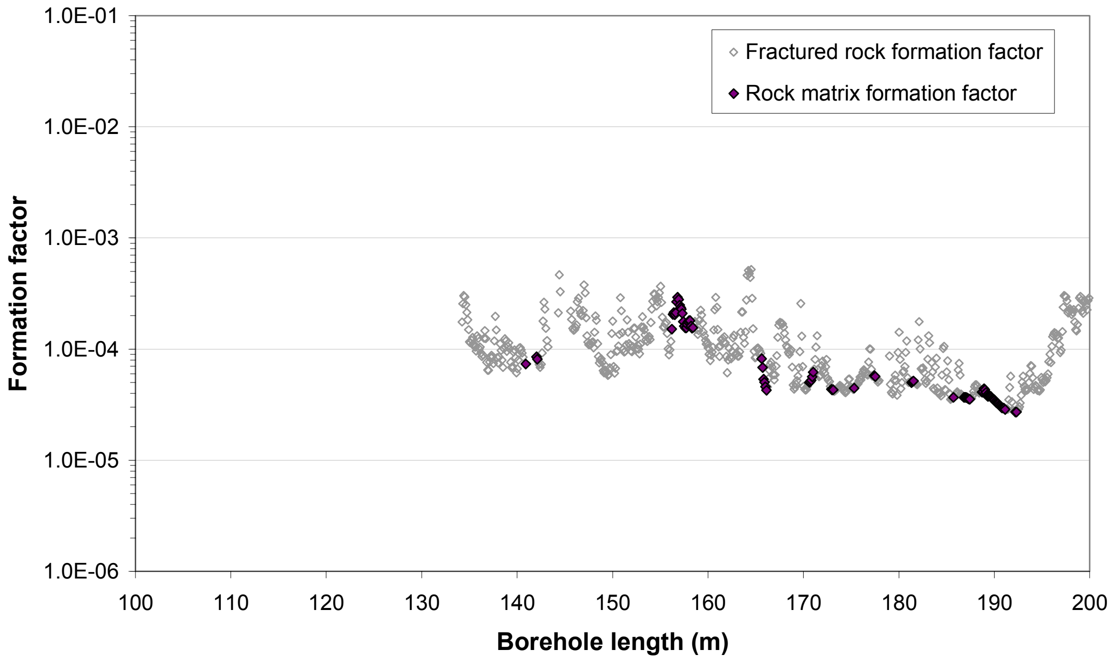

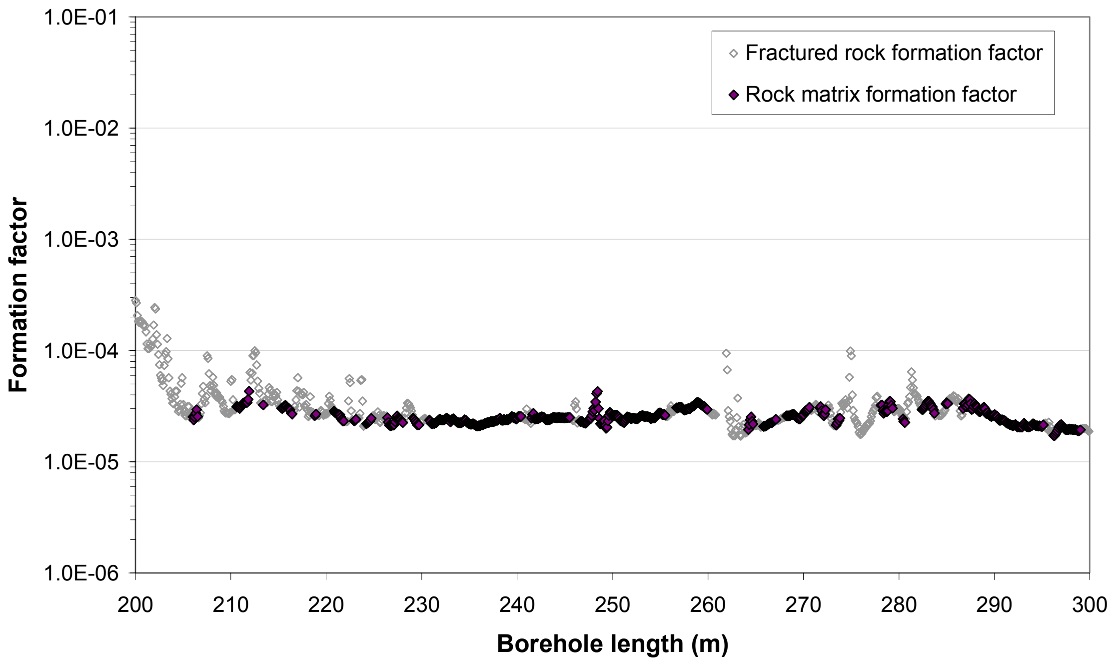

Appendix B1: **In-situ formation factors KFM07A**

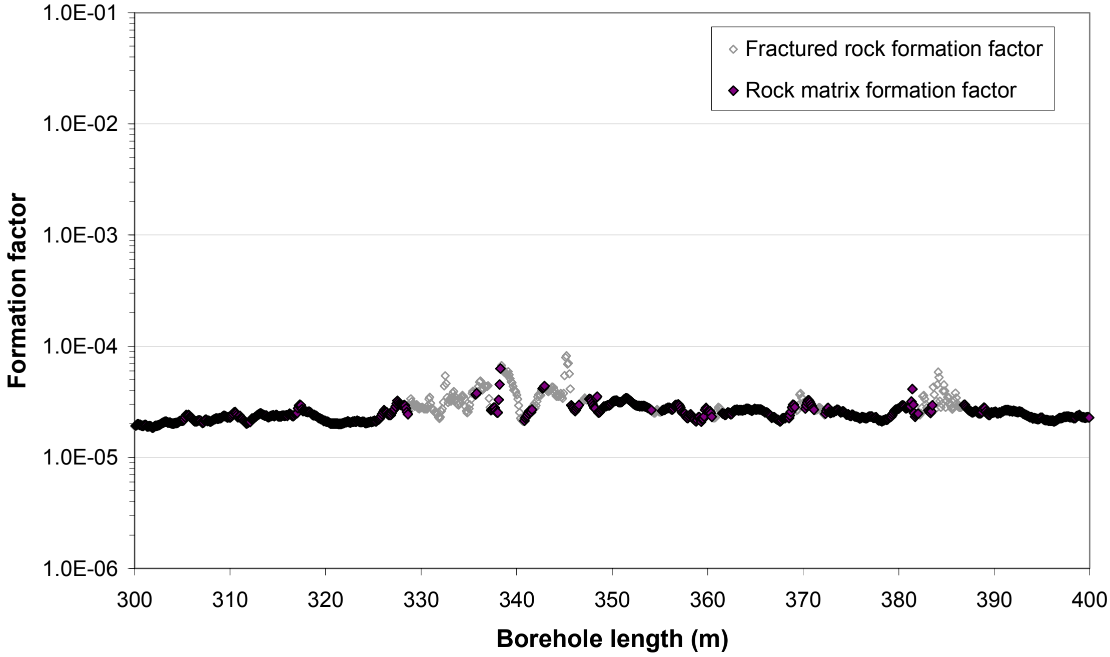

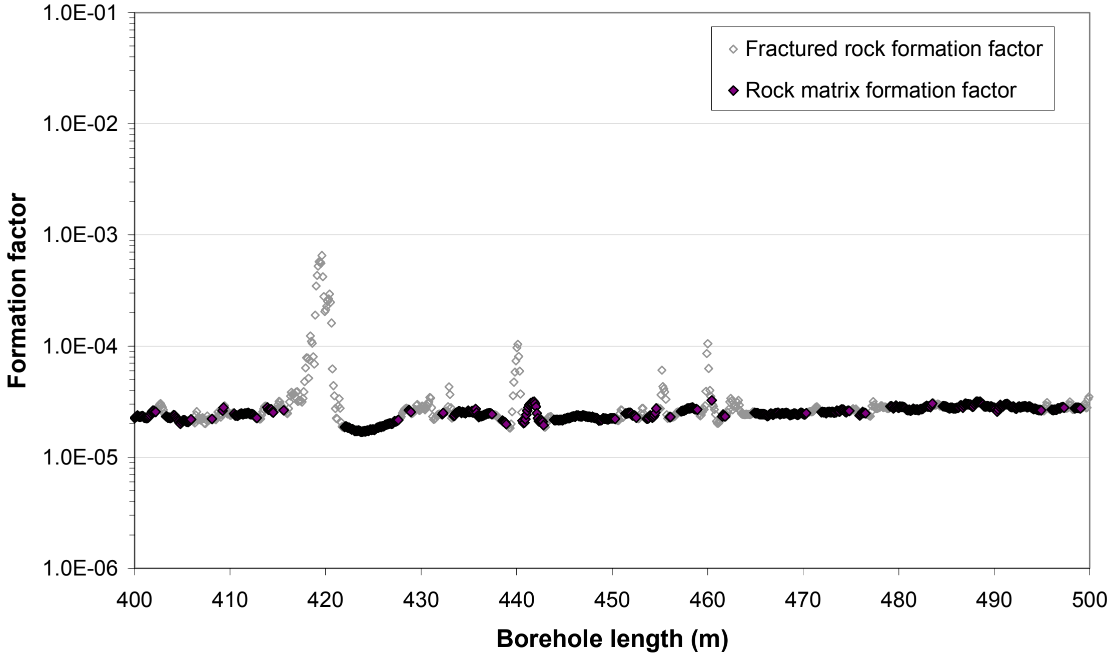

Appendix B1: **In-situ formation factors KFM07A**

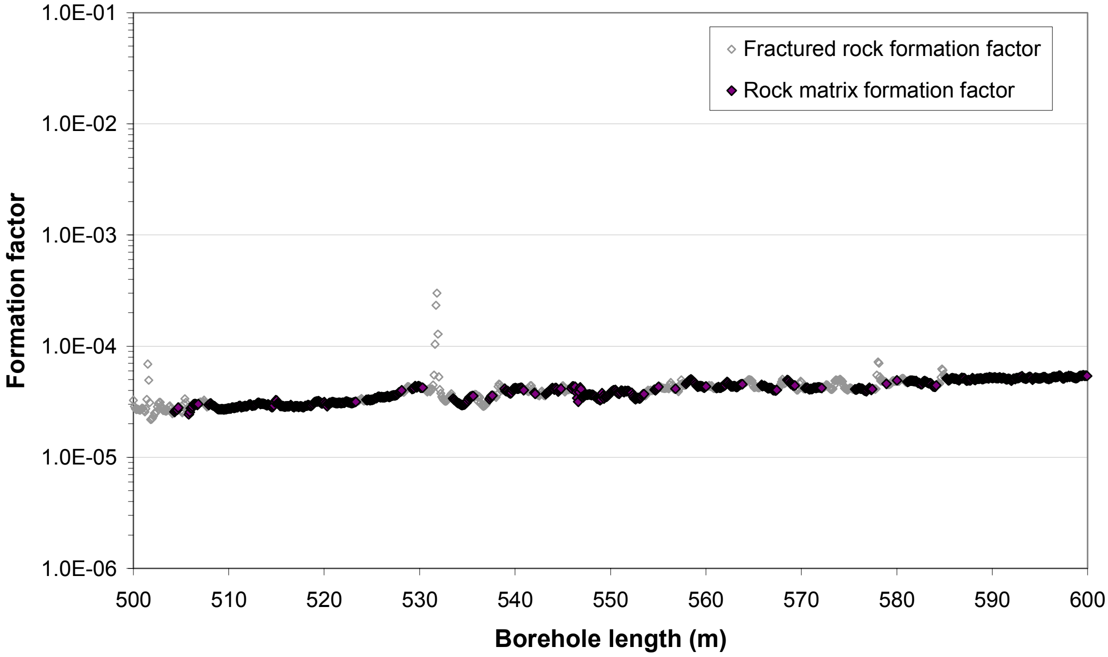

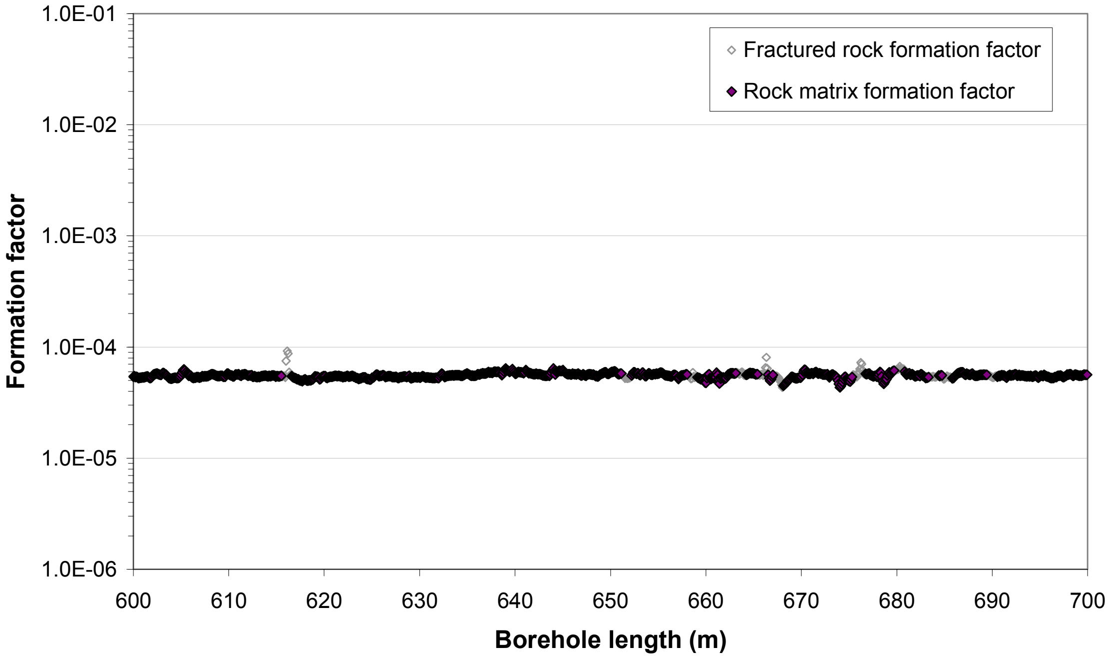

Appendix B1: **In-situ formation factors KFM07A**

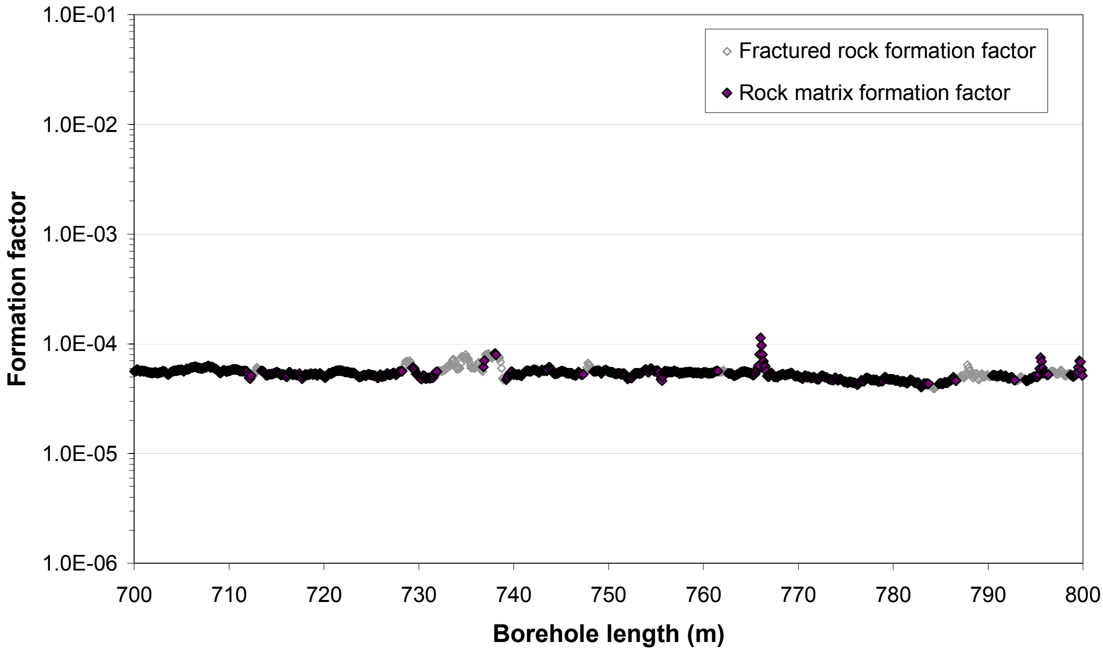

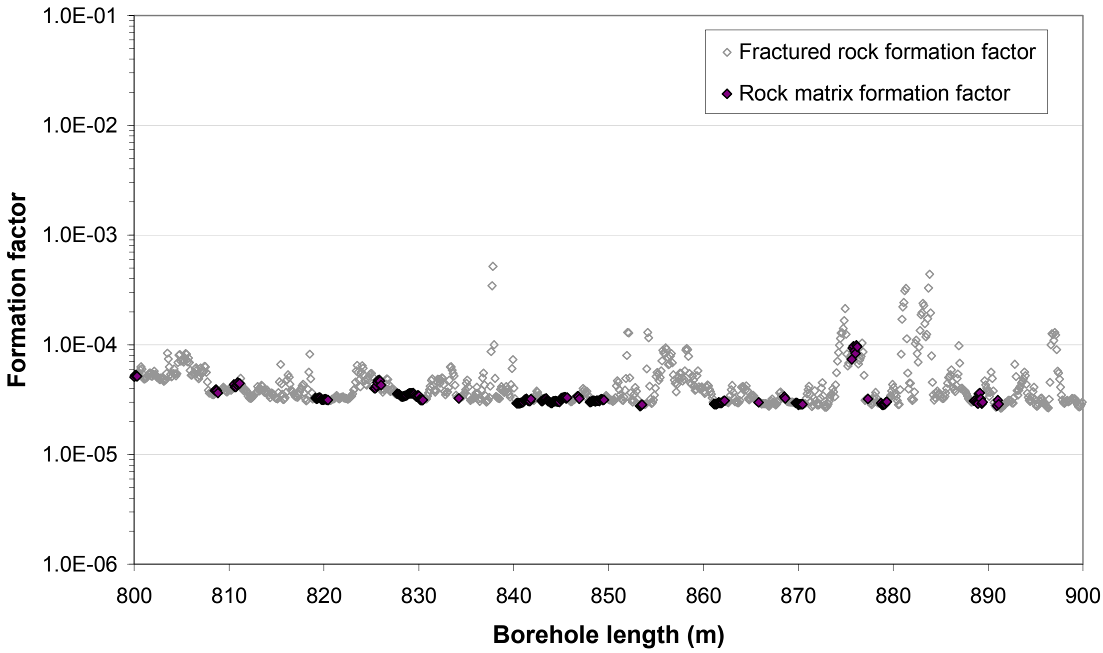

Appendix B1: **In-situ formation factors KFM07A**

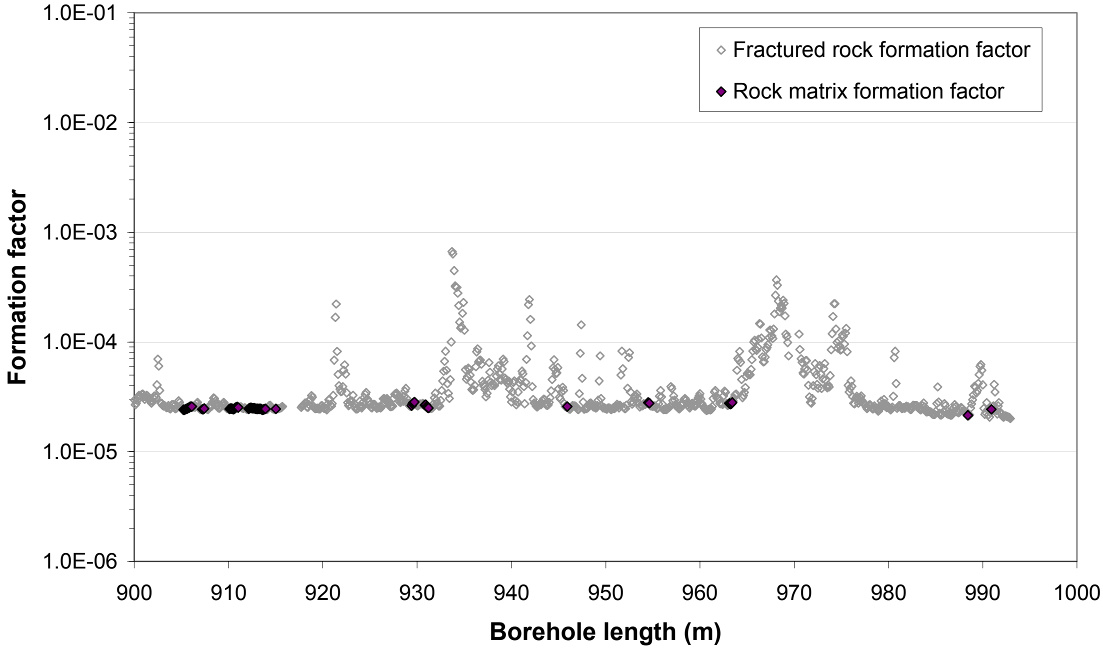

Appendix B2. In situ formation factors KFM08A

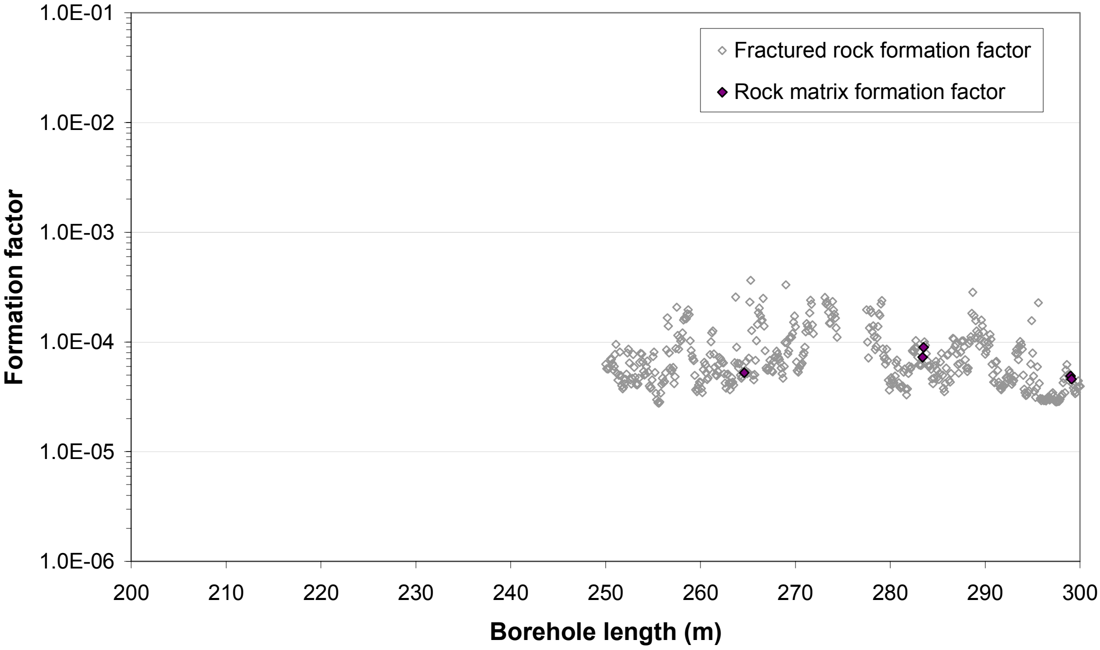

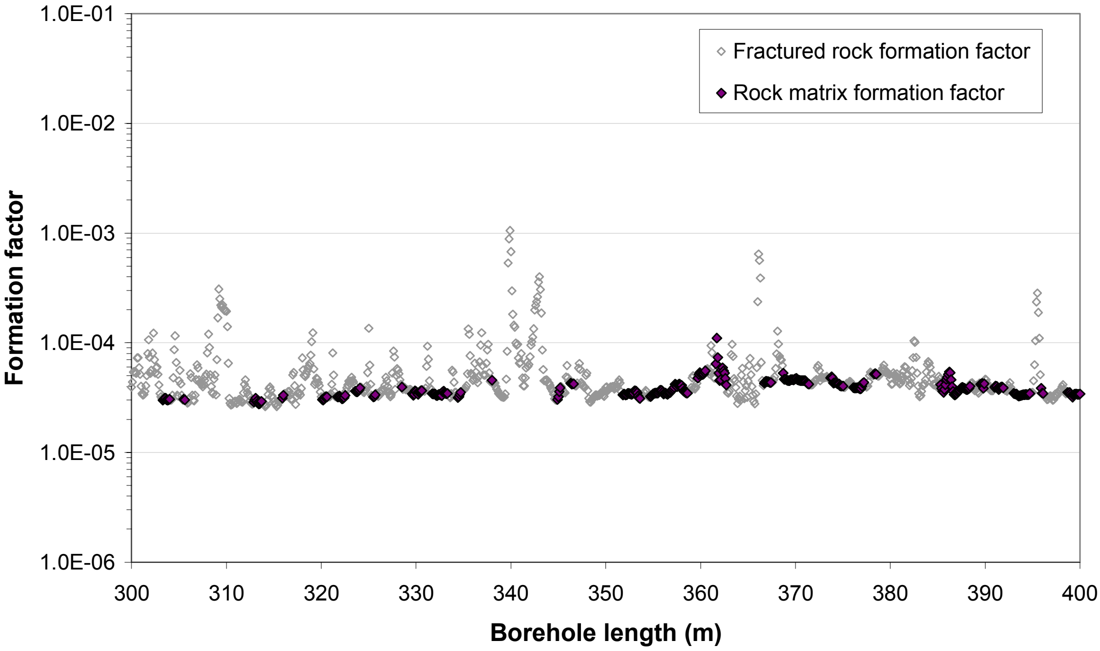

Appendix B2: **In-situ formation factors KFM08A**

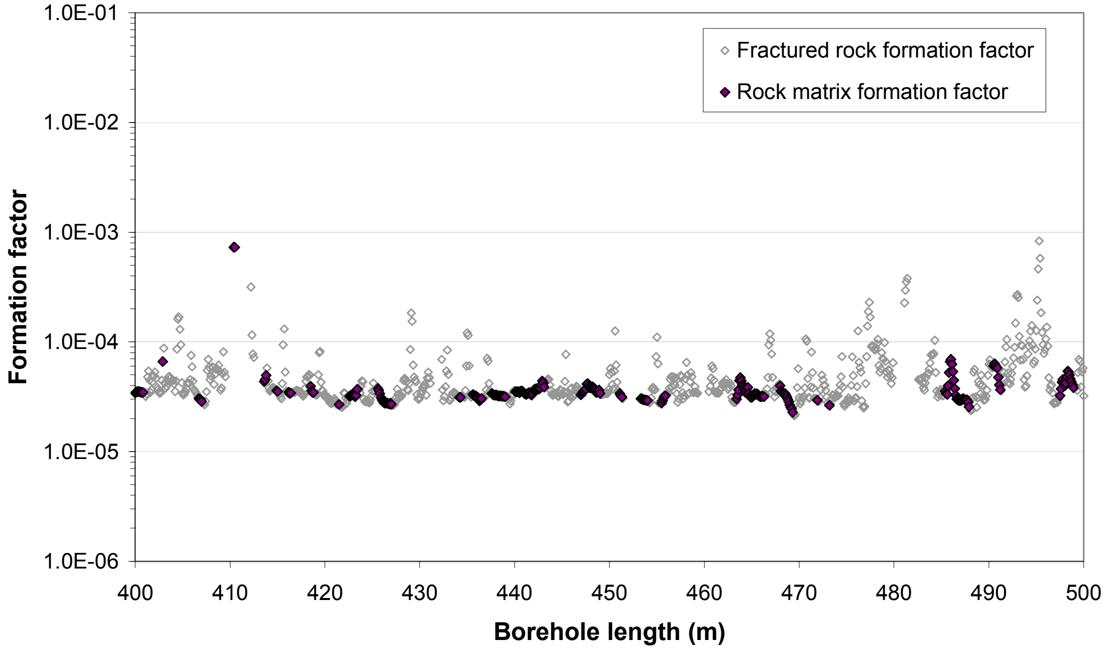

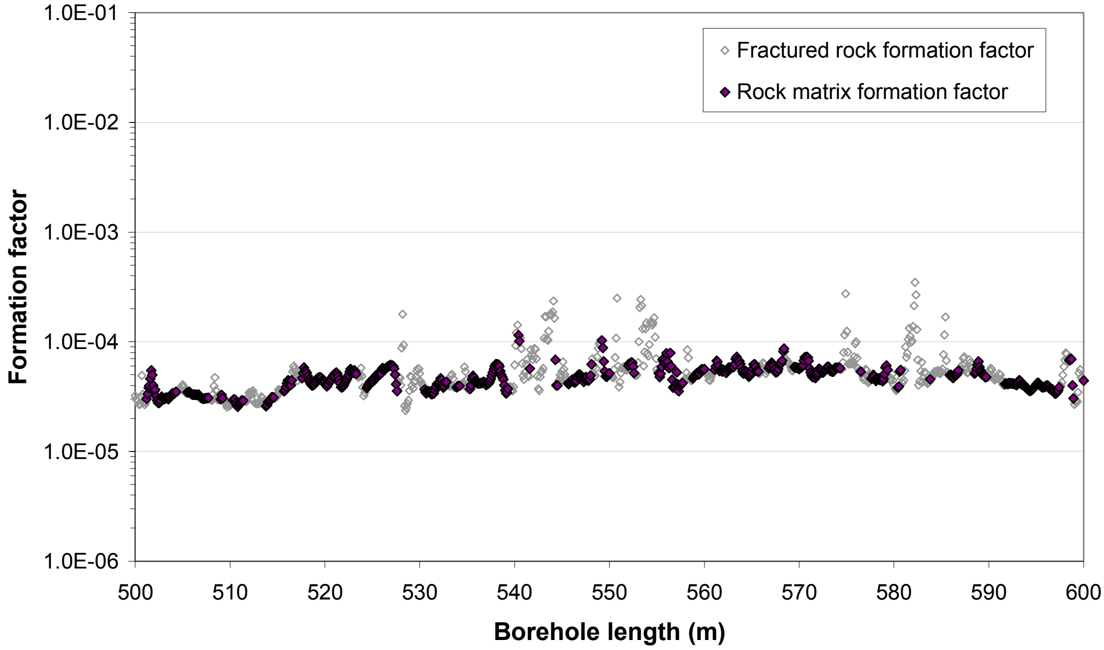

Appendix B2: **In-situ formation factors KFM08A**

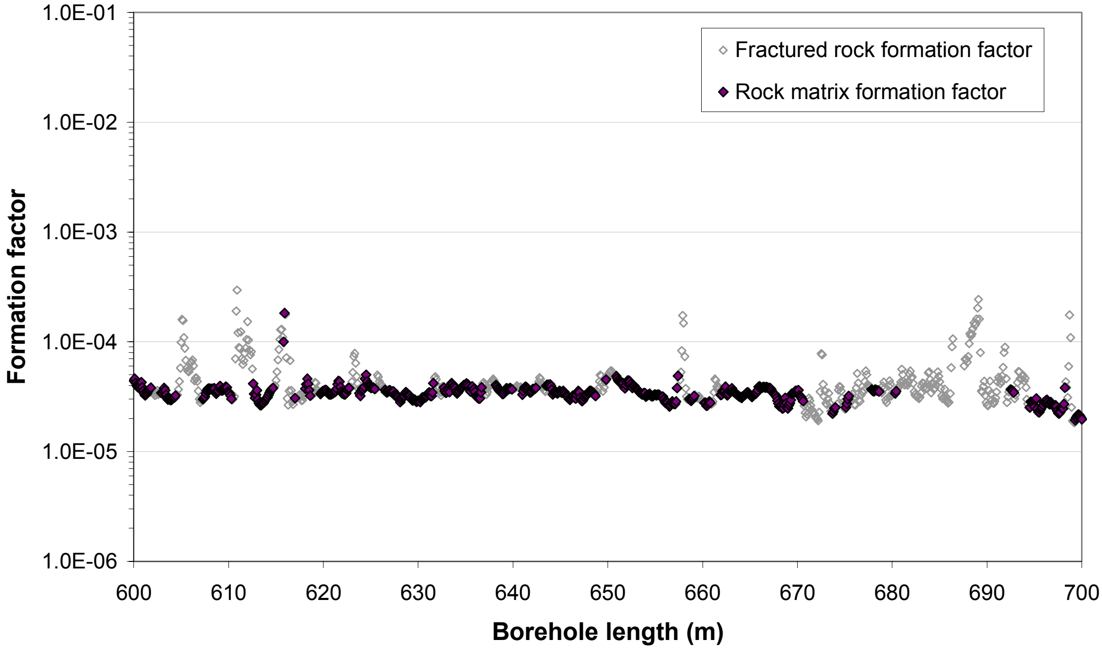

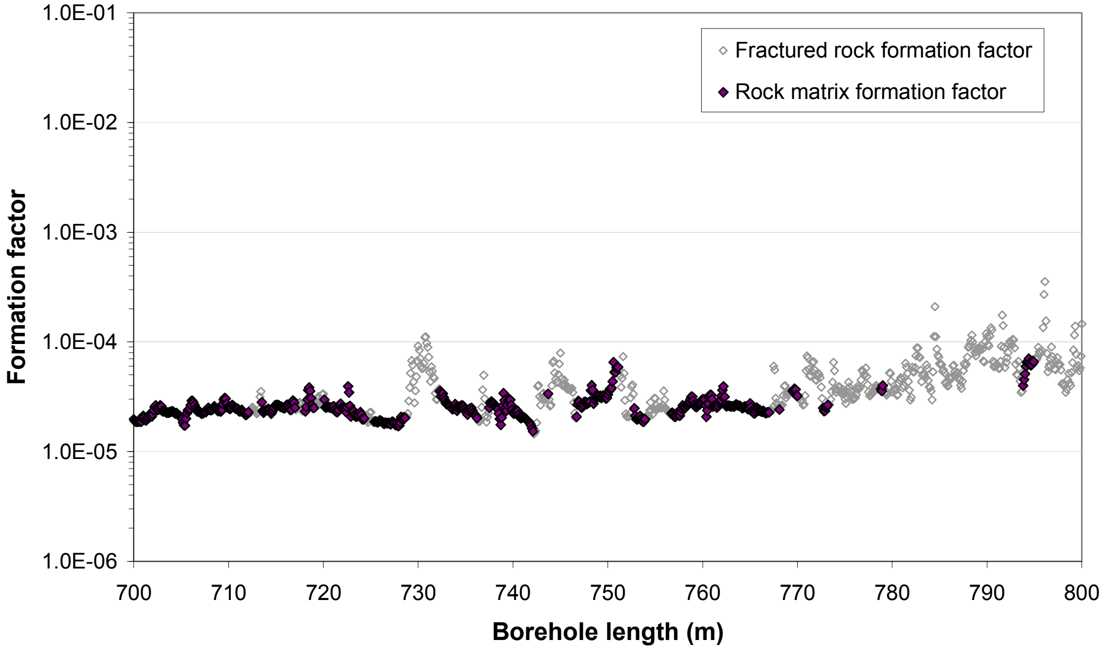

Appendix B2: **In-situ formation factors KFM08A**

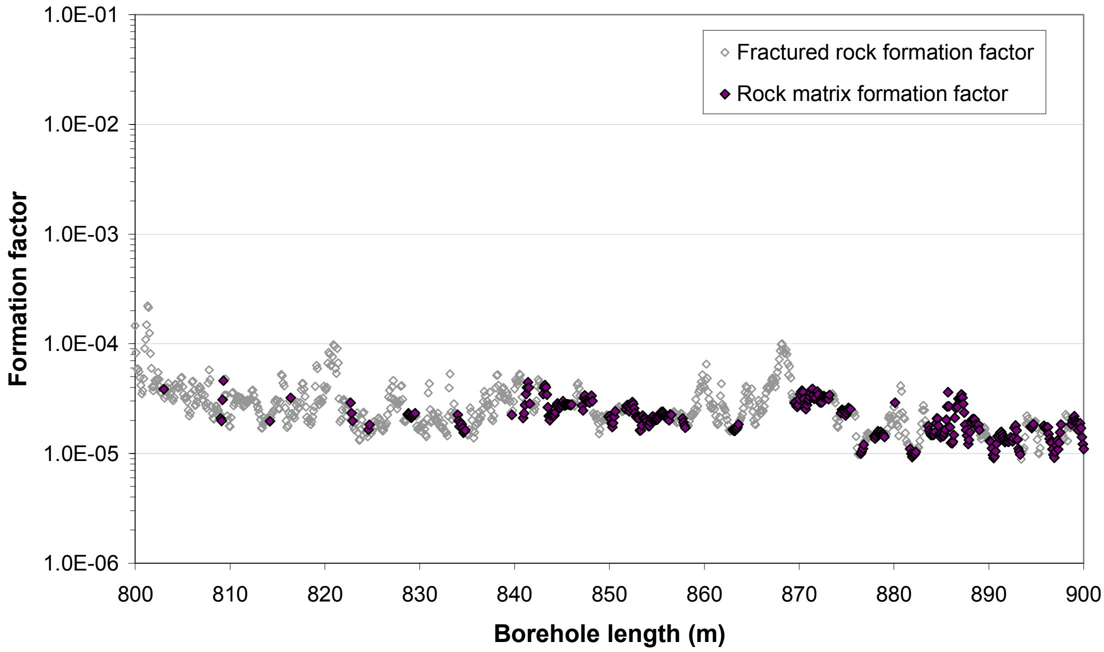

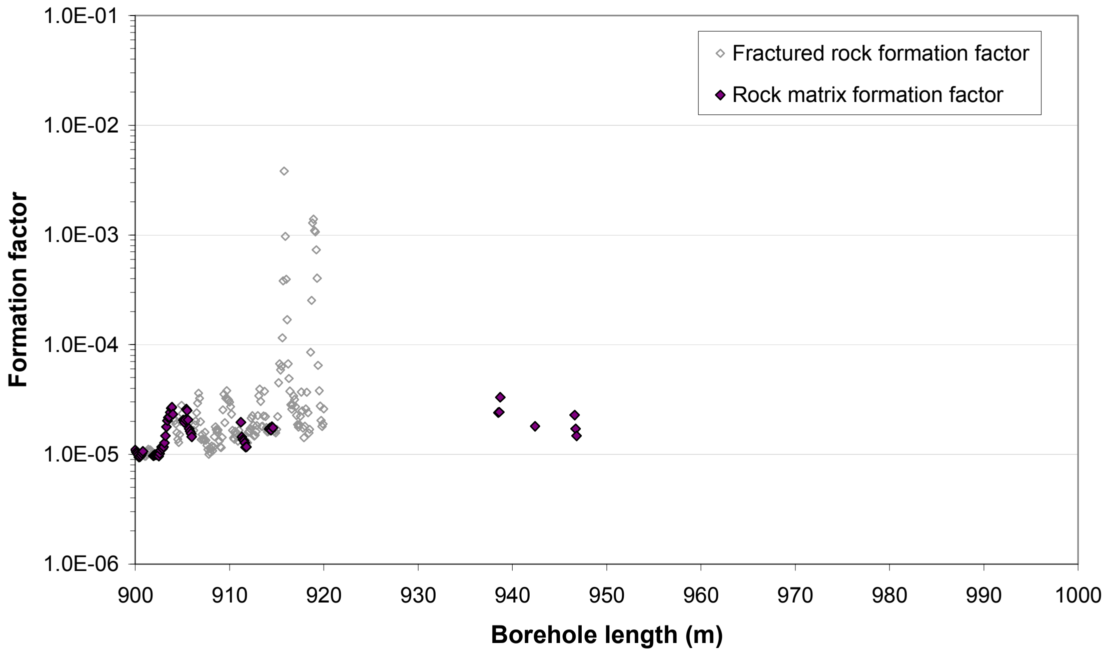

Appendix C

Groundwater EC data Forsmark

Borehole	Inclination	Borehole length	Borehole depth	EC 25°C	EC in situ	Method
KFM01A	84.7°	116.0	115.5	1.52	1.01	HC
		178.0	177.2	1.55	1.05	HC
KFM02A	84.7°	110.7	110.2	0.22	0.15	Diff
		111.1	110.6	0.22	0.15	Diff
		112.9	112.4	0.16	0.11	Diff
		114.2	113.7	0.18	0.12	Diff
		116.6	116.1	0.14	0.09	Diff
		117.5	117.0	0.15	0.10	Diff
		118.3	117.8	0.12	0.08	Diff
		119.0	118.5	0.12	0.08	Diff
		120.9	120.4	0.35	0.23	Diff
		121.1	120.5	0.41	0.27	Diff
		162.8	162.1	1.3	0.87	Diff
		171.7	171.0	1.2	0.81	Diff
		426.8	425.0	1.6	1.15	Diff
		513.6	511.4	1.6	1.17	Diff
KFM03A	85.8°	388.6	387.5	2.34	1.67	Diff
		388.6	387.5	1.65	1.17	Diff
		451.3	450.0	2.28	1.65	Diff
		451.3	450.0	1.63	1.18	Diff
		643.9	642.1	2.28	1.72	Diff
		643.9	642.1	1.62	1.23	Diff
		643.9	642.1	1.61	1.22	Diff
		944.2	941.5	3.29	2.66	Diff
		944.2	941.5	2.31	1.87	Diff
		986.4	983.6	3.84	3.14	Diff
		986.4	983.6	2.89	2.36	Diff
KFM04A	60.1°	116.3	100.8	0.87	0.58	Diff
		207.1	179.5	1.4	0.95	Diff
		235.6	204.2	1.46	0.99	Diff
		297.1	257.6	1.48	1.02	Diff
		359.8	311.9	1.45	1.01	Diff
KFM05A	59.8°	116.5	100.7	1.56	1.04	Diff
		124.3	107.4	1.54	1.02	Diff
		175.6	151.8	1.44	0.97	Diff
		264.4	228.5	1.41	0.97	Diff
		720.0	622.3	1.38	1.04	HC
KFM06A	60.3°	126.0	109.44	1.18	0.78	Diff
		128.7	111.79	1.38	0.91	Diff
		129.2	112.18	1.46	0.97	Diff
		130.3	113.18	1.46	0.97	Diff

Borehole	Inclination	Borehole length	Borehole depth	EC 25°C	EC in situ	Method
		131.9	114.52	1.44	0.96	Diff
		135.2	117.43	1.43	0.95	Diff
		177.4	154.09	1.51	1.02	Diff
		181.1	157.30	1.49	1.00	Diff
		218.2	189.53	1.46	0.99	Diff
		238.0	206.73	1.48	1.01	Diff
		268.6	233.31	1.43	0.98	Diff
		269.3	233.91	1.45	0.99	Diff
		356.6	309.74	1.17	0.81	Diff
		743.3	645.63	1.36	1.03	Diff
		355.4	308.70	1.34	0.93	HC
		770.7	669.43	1.95	1.49	HC

Based on Appendix D in /12/. For further information /12/ is recommended.

Borehole	Inclination	Borehole length	Borehole depth	EC 25°C	EC in situ	Method
KFM07A	59.22	133.7	114.8	1.19	0.79	Diff
		178.5	153.3	1.44	0.96	Diff
		261.4	224.5	2.65	1.81	Diff
		934	802	3.63	3.0	HC
		970.0	833.1	3.7	3.1	Diff
KFM08A	58.85	189.8	162.9	0.62	0.41	Diff
		190.5	163.5	0.62	0.41	Diff
		275.1	236.2	0.86	0.58	Diff
		480.5	412.5	1.09	0.77	Diff
		687.0	589.8	1.34	1.00	Diff

Based on Table 4-6 and 4-7. Inclination is inclination at ground surface /1/.
Diff: Difference flow meter, HC: Hydrochemical characterisation